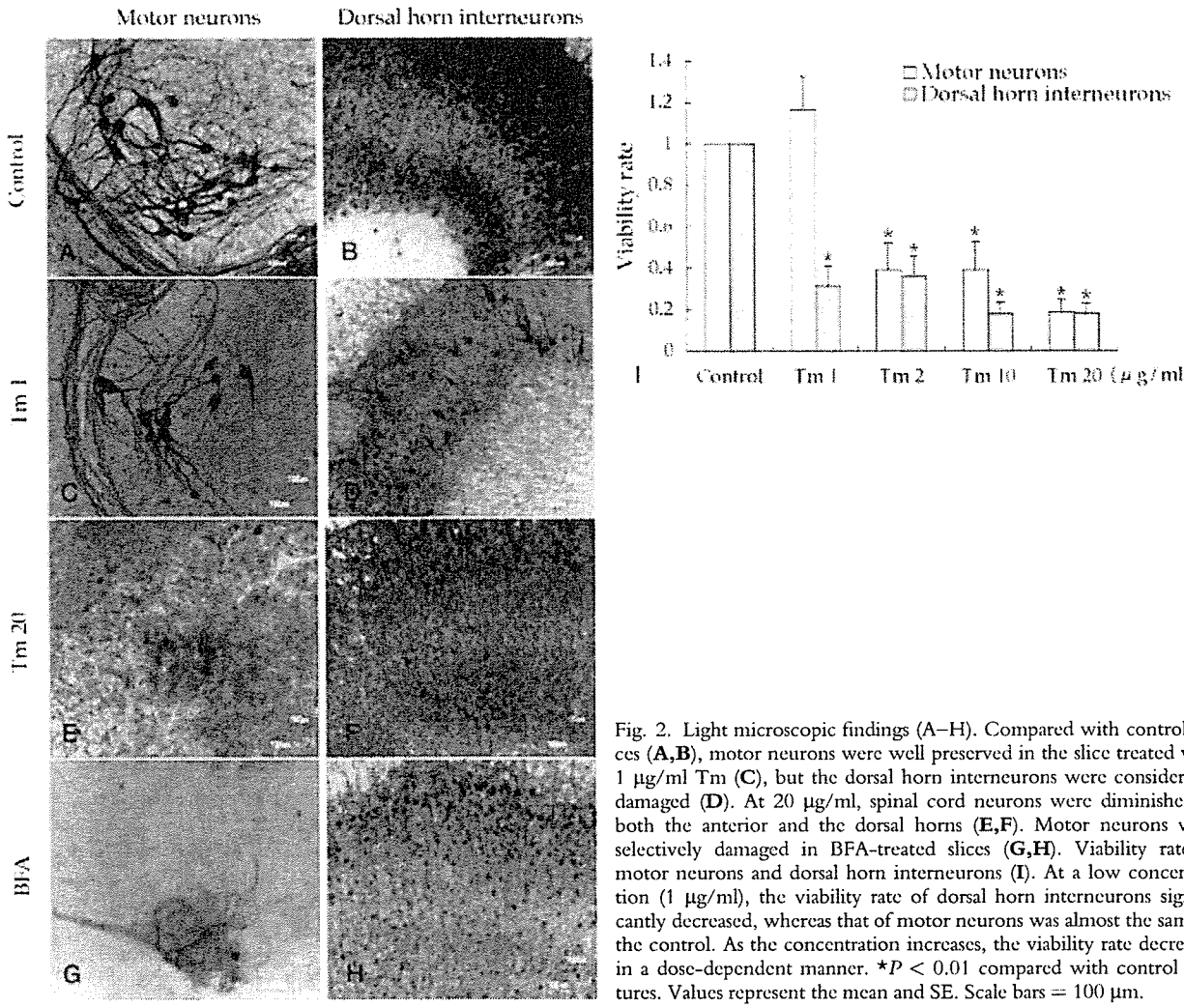

Fig. 2. Light microscopic findings (A–H). Compared with control slices (**A,B**), motor neurons were well preserved in the slice treated with 1 μg/ml Tm (**C**), but the dorsal horn interneurons were considerably damaged (**D**). At 20 μg/ml, spinal cord neurons were diminished in both the anterior and the dorsal horns (**E,F**). Motor neurons were selectively damaged in BFA-treated slices (**G,H**). Viability rate of motor neurons and dorsal horn interneurons (**I**). At a low concentration (1 μg/ml), the viability rate of dorsal horn interneurons significantly decreased, whereas that of motor neurons was almost the same as the control. As the concentration increases, the viability rate decreased in a dose-dependent manner. $*P < 0.01$ compared with control cultures. Values represent the mean and SE. Scale bars = 100 μm.

concentration of Tm was a high 20 μg/ml. The viability rate of motor neurons also increased with addition of PFT, but the difference was not statistically significant at any concentration of Tm tested.

Accumulation of p53 in the Dorsal Horn After Tm Treatment

Immunofluorescence analysis of slices cultured with Tm showed p53 immunoreactivity, which was considered to be p53-nuclear accumulation, in the dorsal horn area after double staining with antibodies for p53 and calretinin (Fig. 4). Calretinin-positive dorsal horn interneurons markedly decreased in Tm-treated slices and were not superimposed on p53-positive spots in a merged image. These findings suggest that the dorsal horn interneurons with nuclear translocation of p53 were too severely damaged to retain immunoreactivity for anticalretinin antibodies. In the anterior horns of Tm-treated slices, there was weak p53 staining of the cytosol of a motor neuron, but no definite evidence of nuclear accumulation. Control slices did not show any clear p53 staining in either the anterior horn or the dorsal horn. We also performed an immunofluorescence study with Hoechst 33258, but the background staining was too high for proper interpretation, and we could not determine whether apoptosis was involved in the neuronal death.

DISCUSSION

In the present study, Tm was shown to induce ER stress and spinal cord neurotoxicity, but it was not selective for motor neurons. Rather, dorsal horn interneurons were more vulnerable than motor neurons, which is inconsistent with the results of our previous study using

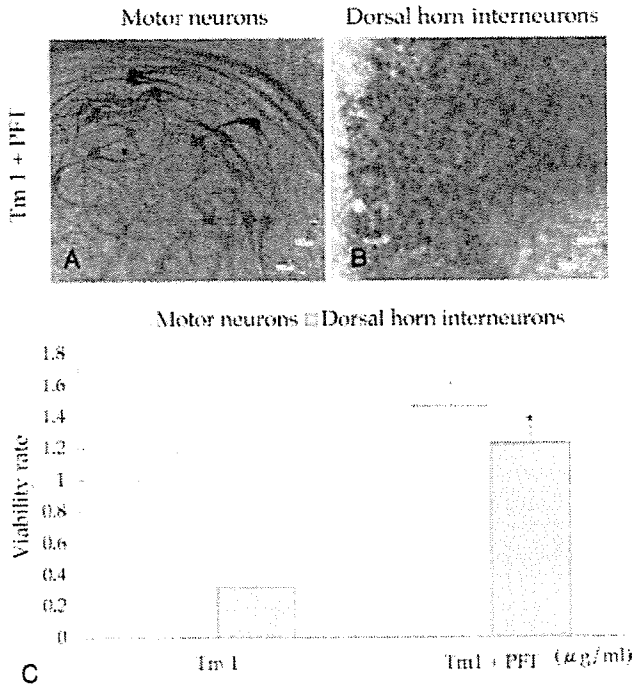

Fig. 3. Protective effect of PFT against neurotoxicity induced by 1 μg/ml Tm (**A,B**). The viability rate of the dorsal horn interneurons significantly increased in slices treated concomitantly with 1 μg/ml Tm and PFT (**C**). The viability rate of motor neurons did not significantly increase with PFT at any concentration of Tm (C). $*P < 0.01$. Values represent the mean and SE. Scale bars = 100 μm.

BFA as an ER stress inducer for cells in dissociated culture (Kikuchi et al., 2003). Although different experimental systems were used in the two studies, the discrepancy can be attributed to the different ER stress inducers, because BFA also tended to damage neurons in the anterior horn more severely than in the dorsal horn in our organotypic slice culture system.

Both Tm and BFA are potent ER stress inducers, and it is generally considered that they equally induce ER stress in several experimental systems (Nakagawa et al., 2000; Aoki et al., 2002; Shiraishi et al., 2005), but the mechanism causing ER stress is different. Tm inhibits protein N-linked glycosylation inside the ER, whereas BFA blocks protein transport from the ER to the Golgi apparatus. This difference in action can have various consequences, as we have shown in the present study. Even when both Tm and BFA exert the same effect on one cell type, their effects on another cell type might not always be the same (Ledesma et al., 2002).

In general, various kinds of stress acting on the ER cause the UPR, and, when cells cannot cope with the stress, apoptosis occurs via several signaling pathways. We used a p53 inhibitor to examine whether p53 was involved in ER-stress induced apoptosis, because there is accumulating evidence for the contribution of p53 to the stress-signaling pathways leading to neuronal death. A p53 inhibitor, PFT, was effective at protecting dorsal horn interneurons from Tm neurotoxicity in this study. In addition, immunofluorescence showed nuclear accumulation of p53 in the dorsal horns of slices treated with Tm. Thus, the induction of dorsal horn neuronal damage by Tm was shown to be p53 dependent.

p53 Is a well-known tumor suppressor gene product, and its antitumor activity is achieved primarily through the induction of apoptosis (Schmitt et al., 2002). The mechanisms by which p53 induces apoptosis are both transcription dependent and independent (Fridman and Lowe, 2003; Fig. 5). After activation, p53 translocates to the nucleus and initiates the transcription of various proapoptotic factors that include death receptors, Bcl-2 proteins such as Bax, the BH3-only proteins Bid and Noxa, and p53 up-regulated modulation of apoptosis (PUMA; Culmsee and Mattson, 2005). p53 Also accumulates in the cytoplasm, where it mediates mitochondrial outer membrane permeabilization through direct physical interaction with Bax in a transcription-independent manner (Chipuk et al., 2004). After the mitochondrial outer membrane permeabilization occurs, factors such as cytochrome c and apoptosis-inducing factor (AIF) are released to activate caspase-dependent and -independent cell death processes, respectively (Hong et al., 2004).

PFT is a synthetic, cell-permeable p53 inhibitor that mainly inhibits translocation of p53 into the nucleus (Culmsee and Mattson, 2005). PFT was originally isolated for its ability to reversibly block p53-dependent transcriptional activation and apoptosis (Komarov et al., 1999). It has been shown that PFT suppresses the transactivation of p53-responsive genes encoding p21, Mdm2, cyclin G, and Bax, and the antiapoptotic effect of PFT has been found to be p53-dependent (Gudkov and Komarova, 2005). Also, PFT lowers the nuclear, but not cytoplasmic, level of p53 protein after DNA damage (Komarov et al., 1999). Taken together, these observations suggest that the major mechanism by which PFT protects against apoptosis is the inhibition of p53 nuclear translocation (Fig. 5).

Our results suggest that p53 nuclear translocation plays the central role in the mechanism leading to Tm-induced death of dorsal horn interneurons, which provides strong support for those earlier reports. On the other hand, the viability rate of motor neurons did not significantly increase by PFT, and p53 nuclear accumulation was not found in the anterior horns of Tm-treated slices. These findings indicate that p53 nuclear translocation might not be primarily involved in Tm-induced motor neuronal death. A study using several tumor cell lines demonstrated that ER stress inhibited p53-mediated apoptosis through the increased cytoplasmic localization of p53 (Qu et al., 2004). This indicates that the actions of p53 may depend on the cell type and that motor neurons might have different mechanisms for coping with various cellular stresses compared with other neurons.

With regard to the mechanisms of Tm-induced dorsal horn interneuronal death, the downstream path-

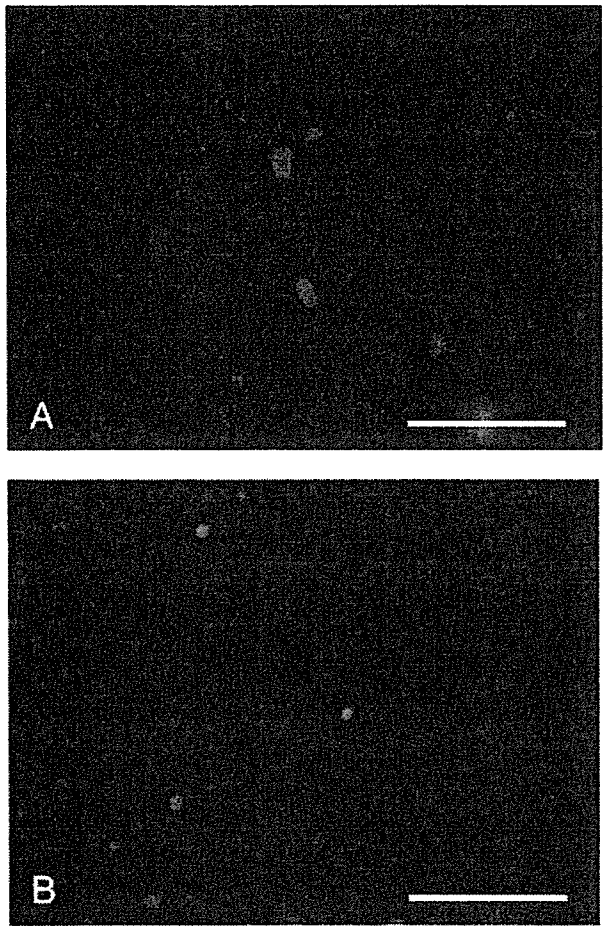

Fig. 4. Immunofluorescence micrographs of a dorsal horn doubly stained with anticalretinin antibody (**A**) and anti-p53 monoclonal antibody (**B**). Dorsal horn interneurons were severely damaged (A), and nuclear accumulation of p53 is seen in the dorsal horn of a slice treated with Tm (B). Control slices showed no p53 immunoreactivity in either the anterior horn or the dorsal horn (not shown). Scale bars = 100 μm.

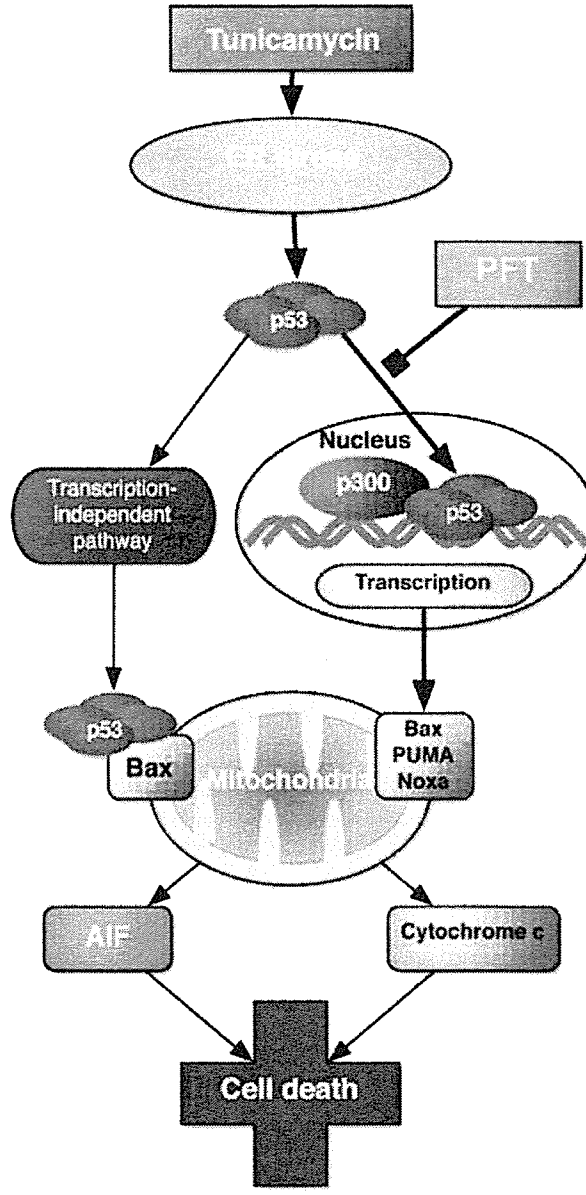

Fig. 5. Diagram of the pathways that may be involved in Tm-induced neuronal death. In the present study, PFT was significantly effective at ameliorating Tm-induced dorsal horn interneuronal toxicity, and nuclear accumulation of p53 was demonstrated by immunofluorescence, suggesting that the nuclear translocation of p53 was necessary for Tm to kill dorsal horn interneurons. Motor neurons may be damaged via different mechanisms, including a p53 transcription-independent pathway, because these cells were not effectively protected by PFT.

ways after the translocation of p53 to the nucleus have not been demonstrated in the present study. As well as the contribution of caspase cascade to this process, the involvement of apoptosis in the dorsal horn interneuronal death itself remains to be clarified. We are working on these issues to reveal the network of the pathways leading to ER-stress-induced neuronal death.

In conclusion, the present study has shown that dorsal horn interneurons were more vulnerable to Tm-induced neurotoxicity than motor neurons in organotypic slice cultures of rat spinal cord and that this toxicity was effectively attenuated by PFT, suggesting the involvement of p53 in Tm-induced dorsal horn interneuronal death. We could not detect a significant protective effect of PFT against motor neuronal death, but the difference between dorsal horn interneurons and motor neurons may be a clue to a better understanding of the stress-response pathways. Moreover, a better understanding of the pathways involved might allow p53 inhibitors to be used in the treatment of spinal cord conditions,

such as ischemia and injury, or demyelinating and neurodegenerative diseases, including ALS.

REFERENCES

Aoki S, Su Q, Li H, Nishikawa K, Ayukawa K, Hara Y, Namikawa K, Kiryu-Seo S, Kiyama H, Wada K. 2002. Identification of an axotomy-induced glycosylated protein, AIGP1, possibly involved in cell death triggered by endoplasmic reticulum-Golgi stress. J Neurosci 22:10751–10760.

Chipuk JE, Kuwana T, Bouchier-Hayes L, Droin NM, Newmeyer DD, Schuler M, Green DR. 2004. Direct activation of Bax by p53 mediates mitochondrial membrane permeabilization and apoptosis. Science 303: 1010–1014.

Culmsee C, Mattson MP. 2005. p53 In neuronal apoptosis. Biochem Biophys Res Commun 331:761–777.

DeGracia DJ, Montie HL. 2004. Cerebral ischemia and the unfolded protein response. J Neurochem 91:1–8.

Fridman JS, Lowe SW. 2003. Control of apoptosis by p53. Oncogene 22:9030–9040.

Fujita Y, Okamoto K. 2005. Golgi apparatus of the motor neurons in patients with amyotrophic lateral sclerosis and in mice models of amyotrophic lateral sclerosis. Neuropathology 25:388–394.

Gudkov AV, Komarova EA. 2005. Prospective therapeutic applications of p53 inhibitors. Biochem Biophys Res Commun 331:726–736.

Hervias I, Beal MF, Manfredi G. 2005. Mitochondrial dysfunction and amyotrophic lateral sclerosis. Muscle Nerve [E-pub ahead of print].

Hetz C, Russelakis-Carneiro M, Maundrell K, Castilla J, Soto C. 2003. Caspase-12 and endoplasmic reticulum stress mediate neurotoxicity of pathological prion protein. EMBO J 22:5435–5445.

Hong SJ, Dawson TM, Dawson VL. 2004. Nuclear and mitochondrial conversations in cell death: PARP-1 and AIF signaling. Trends Pharmacol Sci 25:259–264.

Katayama T, Imaizumi K, Manabe T, Hitomi J, Kudo T, Tohyama M. 2004. Induction of neuronal death by ER stress in Alzheimer's disease. J Chem Neuroanat 28:67–78.

Kaufman RJ. 1999. Stress signaling from the lumen of the endoplasmic reticulum: coordination of gene transcriptional and translational controls. Genes Dev 13:1211–1233.

Kheradpezhouh M, Shavali S, Ebadi M. 2003. Salsolinol causing Parkinsonism activates endoplasmic reticulum-stress signaling pathways in human dopaminergic SK-N-SH cells. Neurosignals 12:315–324.

Kikuchi S, Shinpo K, Takeuchi M, Tsuji S, Yabe I, Niino M, Tashiro K. 2002. Effect of geranylgeranylaceton on cellular damage induced by proteasome inhibition in cultured spinal neurons. J Neurosci Res 69: 373–381.

Kikuchi S, Shinpo K, Tsuji S, Yabe I, Niino M, Tashiro K. 2003. Brefeldin A-induced neurotoxicity in cultured spinal cord neurons. J Neurosci Res 71:591–599.

Komarov PG, Komarova EA, Kondratov RV, Christov-Tselkov K, Coon JS, Chernov MV, Gudkov AV. 1999. A chemical inhibitor of p53 that protects mice from the side effects of cancer therapy. Science 285:1733–1737.

Ledesma MD, Galvan C, Hellias B, Dotti C, Jensen PH. 2002. Astrocytic but not neuronal increased expression and redistribution of parkin during unfolded protein stress. J Neurochem 83:1431–1440.

Liu CY, Kaufman RJ. 2003. The unfolded protein response. J Cell Sci 116:1861–1862.

Nakagawa T, Zhu H, Morishima N, Li E, Xu J, Yankner BA, Yuan J. 2000. Caspase-12 mediates endoplasmic-reticulum-specific apoptosis and cytotoxicity by amyloid-beta. Nature 403:98–103.

Nishitoh H, Matsuzawa A, Tobiume K, Saegusa K, Takeda K, Inoue K, Hori S, Kakizuka A, Ichijo H. 2002. ASK1 is essential for endoplasmic reticulum stress-induced neuronal cell death triggered by expanded polyglutamine repeats. Genes Dev 16:1345–1355.

Paschen W, Frandsen A. 2001. Endoplasmic reticulum dysfunction—a common denominator for cell injury in acute and degenerative diseases of the brain? J Neurochem 79:719–725.

Paschen W, Mengesdorf T. 2005. Endoplasmic reticulum stress response and neurodegeneration. Cell Calcium 38:409–415.

Qu L, Huang S, Baltzis D, Rivas-Estilla AM, Pluquet O, Hatzoglou M, Koumenis C, Taya Y, Yoshimura A, Koromilas AE. 2004. Endoplasmic reticulum stress induces p53 cytoplasmic localization and prevents p53-dependent apoptosis by a pathway involving glycogen synthase kinase-3beta. Genes Dev 18:261–277.

Rosen DR, Siddique T, Patterson D, Figlewicz DA, Sapp P, Hentati A, Donaldson D, Goto J, O'Regan JP, Deng HX, Rahmani Z, Krizus A, McKenna-Yasek D, Cayabyab A, Gaston SM, Berger R, Tanzi RE, Halperin JJ, Herzfeldt B, Van den Bergh R, Hung WY, Bird T, Deng G, Mulder DW, Smyth C, Laing NG, Soriano E, Pericak-Vance MA, Haines J, Rouleau GA, Gusella JS, Horvitz HR, Brown RH Jr. 1993. Mutations in Cu/Zn superoxide dismutase gene are associated with familial amyotrophic lateral sclerosis. Nature 362:59–62.

Schmitt CA, Fridman JS, Yang M, Baranov E, Hoffman RM, Lowe SW. 2002. Dissecting p53 tumor suppressor functions in vivo. Cancer Cell 1:289–298.

Shen X, Zhang K, Kaufman RJ. 2004. The unfolded protein response—a stress signaling pathway of the endoplasmic reticulum. J Chem Neuroanat 28:79–92.

Shiraishi T, Yoshida T, Nakata S, Horinaka M, Wakada M, Mizutani Y, Miki T, Sakai T. 2005. Tunicamycin enhances tumor necrosis factor-related apoptosis-inducing ligand-induced apoptosis in human prostate cancer cells. Cancer Res 65:6364–6370.

Swanton E, Holland A, High S, Woodman P. 2005. Disease-associated mutations cause premature oligomerization of myelin proteolipid protein in the endoplasmic reticulum. Proc Natl Acad Sci U S A 102: 4342–4347.

Takahashi R, Imai Y. 2003. Pael receptor, endoplasmic reticulum stress, and Parkinson's disease. J Neurol 250(Suppl 3):III/25–III/29.

Takahashi R, Imai Y, Hattori N, Mizuno Y. 2003. Parkin and endoplasmic reticulum stress. Ann NY Acad Sci 991:101–106.

Tessitore A, Martin MP, Sano R, Ma Y, Mann L, Ingrassia A, Laywell ED, Steindler DA, Hendershot LM, d'Azzo A. 2004. GM1-ganglioside-mediated activation of the unfolded protein response causes neuronal death in a neurodegenerative gangliosidosis. Mol Cell 15:753–766.

Tobisawa S, Hozumi Y, Arawaka S, Koyama S, Wada M, Nagai M, Aoki M, Itoyama Y, Goto K, Kato T. 2003. Mutant SOD1 linked to familial amyotrophic lateral sclerosis, but not wild-type SOD1, induces ER stress in COS7 cells and transgenic mice. Biochem Biophys Res Commun 303:496–503.

Tsuji S, Kikuchi S, Shinpo K, Tashiro J, Kishimoto R, Yabe I, Yamagishi S, Takeuchi M, Sasaki H. 2005. Proteasome inhibition induces selective motor neuron death in organotypic slice cultures. J Neurosci Res 82:443–451.

Vattemi G, Engel WK, McFerrin J, Askanas V. 2004. Endoplasmic reticulum stress and unfolded protein response in inclusion body myositis muscle. Am J Pathol 164:1–7.

Wootz H, Hansson I, Korhonen L, Napankangas U, Lindholm D. 2004. Caspase-12 cleavage and increased oxidative stress during motoneuron degeneration in transgenic mouse model of ALS. Biochem Biophys Res Commun 322:281–286.

Zhang K, Kaufman RJ. 2006. The unfolded protein response: a stress signaling pathway critical for health and disease. Neurology 66(Suppl 1): S102–S109.

BRAIN RESEARCH 1087 (2006) 15–27

available at www.sciencedirect.com

SCIENCE DIRECT

www.elsevier.com/locate/brainres

BRAIN RESEARCH

Research Report

The effects of neuronal induction on gene expression profile in bone marrow stromal cells (BMSC)—a preliminary study using microarray analysis

Satoshi Yamaguchi[a,c], *Satoshi Kuroda*[a,*], *Hiroyuki Kobayashi*[a], *Hideo Shichinohe*[a], *Shunsuke Yano*[a], *Kazutoshi Hida*[a], *Kazuyoshi Shinpo*[b], *Seiji Kikuchi*[b], *Yoshinobu Iwasaki*[a]

[a]*Department of Neurosurgery, Hokkaido University Graduate School of Medicine, North 15 West 7, Kita-ku, Sapporo 060-8638, Japan*
[b]*Department of Neurology, Hokkaido University Graduate School of Medicine, Sapporo, Japan*
[c]*Department of Neurosurgery, Hiroshima University Graduate School of Biomedical Sciences, Hiroshima, Japan*

ARTICLE INFO

Article history:
Accepted 26 February 2006
Available online 13 April 2006

Keywords:
Bone marrow stromal cells
Neuronal differentiation
Gene expression profile
Growth factor
Microarray analysis

ABSTRACT

Bone marrow stromal cells (BMSC) have been anticipated as a donor for cell type for transplantation therapy in various neurological disorders. However, their neurogenic capacity still remains undetermined. In this study, we aimed to clarify whether in vitro chemical treatment promotes their neuronal differentiation on the level of gene expression. Mice BMSC were cultured with medium supplemented with DMSO, retinoic acid, and basic fibroblast growth factor, and their morphology and expression of neuronal markers were evaluated. Subsequently, using microarray and RT-PCR techniques, the treatment-induced changes in the gene expression profile were analyzed. After exposure to the medium, the BMSC simulated a neuron-like appearance and increased their immunoreactivity for nestin and Tuj-1. Microarray analysis revealed that the BMSC per se express the multilineage cellular genes, including those associated with the neuron. Chemical treatment significantly decreased the expression of genes related to mesenchymal cells and increased the expression of 5 neuron-associated genes. Microarray and RT-PCR analyses also demonstrated that the BMSC express the genes for several growth factors including NGF-β and BDNF, indicating their therapeutic role in protecting the injured central nervous system. The present results suggest that at least a certain subpopulation of the BMSC have the potential to alter their gene expression profile in response to the surrounding environment and may possibly protect the host tissue by secreting neuroprotective factors.

1. Introduction

There are two stem cell populations in the bone marrow: hematopoietic stem cells, which differentiate into blood cells, and bone marrow stromal cells (BMSC) (Prockop, 1997). It is well known that BMSC are capable of differentiating into mesodermal derivatives such as bone, cartilage, and fatty tissue (Neuhuber et al., 2004; Prockop, 1997; Sekiya et al., 2002). Recent reports have strongly suggested that BMSC may differentiate into neural cells, and it is expected that these

* *Corresponding author*. Fax: +81 11 708 7737.
E-mail address: skuroda@med.hokudai.ac.jp (S. Kuroda).

0006-8993/$ – see front matter © 2006 Elsevier B.V. All rights reserved.
doi:10.1016/j.brainres.2006.02.127

cells will become a source for cell transplantation therapy for central nervous system disorders. Indeed, several reports have suggested that BMSC can differentiate into neurons in vitro (Deng et al., 2001; Jin et al., 2003; Kim et al., 2002; Kohyama et al., 2001; Sanchez-Ramos et al., 2000; Woodbury et al., 2000). In vivo animal experimental studies have also indicated that transplanted BMSC migrate towards areas of injury, express neuronal phenotypes, and show therapeutic benefits in the damaged central nervous system (Chen et al., 2002a; Chopp et al., 2000; Kopen et al., 1999; Lee et al., 2003, 2004; Mahmood et al., 2001; Ohta et al., 2004; Shichinohe et al., 2004; Wu et al., 2003). Although the exact mechanism has not yet been clarified, there have been several hypotheses to explain their therapeutic effects. First, BMSC per se are believed to differentiate into neural cells in the host's brain or spinal cord ('transdifferentiation theory') (Deng et al., 2001; Jin et al., 2003; Kim et al., 2002; Kohyama et al., 2001; Sanchez-Ramos et al., 2000; Woodbury et al., 2000). This theory is based on the findings that BMSC simulate neuron morphology and express specific neuronal proteins after in vitro induction or in vivo transplantation experiments. Recently, transplanted BMSC have also been reported to fuse with host cells and to undergo "transdifferentiation" into host cells ('cell fusion theory') (Terada et al., 2002; Ying et al., 2002). Alternatively, it has been proposed that BMSC secrete certain cytokines that have neurotrophic and/or neuroprotective effects and support the survival of the host cells ('feeder theory') (Chen et al., 2002b; Lou et al., 2003; Wu et al., 2003; Zhong et al., 2003). Although the transdifferentiation theory is quite attractive, there still remain several questions: How is the mesenchymal cell fate of the BMSC oriented to the neuronal lineage? Are their morphological change and expression of neuronal phenotype identical to differentiation into functional neuronal cells? Moreover, very recent studies posed a question about their in vitro differentiation into neurons. Thus, Lu et al. (2004) showed that chemical stimulation with β-mercaptoethanol or dimethylsulfoxide (DMSO)/butylated hydroxyanisol (BHA) induced "neuron-like" pyramidal cell morphology in not only the rat BMSC but also in rat fibroblast, HEK293 cells and rat PC-12 cells, and their fine-cellular extensions mimicking neurites result from cellular shrinkage due to simple chemical toxicity (Lu et al., 2004). Neuhuber et al. (2004) also demonstrated that their morphological change after treatment with the induction medium including DMSO was caused by rapid disruption of the actin cytoskeleton and was not accompanied by gene expression specific for the neurons (Neuhuber et al., 2004).

However, it is critical to determine the exact mechanism by which the transplanted BMSC improve neurological symptoms in order to safely and effectively apply BMSC transplantation therapy to clinical situations. If the BMSC were able to differentiate into neural cells in vitro, they would necessarily alter their gene profile to amend their phenotypes. Similarly, if the BMSC could produce certain neuroprotective or trophic factors, they would express mRNA for those factors.

Based on these considerations, therefore, this study was designed to clarify whether BMSC would alter their gene expression profile and increase the expression of genes specific to neurons in response to in vitro chemical treatments. For this purpose, we exhaustively analyzed their gene expression profile before and after chemical treatments, using microarray and RT-PCR techniques. Simultaneously, we also assessed their gene expression for known neuroprotective or trophic factors.

2. Results

2.1. *Isolation of BMSC and their characterization*

BMSC could be isolated from whole marrow cells by their adherence to the bottom of the flask. The BMSC became relatively homogeneous in appearance as the passages progressed. When the passage reached P3, the cells demonstrated a flat and polygonal-shaped appearance (Fig. 1A). On immunocytochemistry, approximately 8% of the BMSC were positive for nestin, a neuronal precursor cell marker (Fig. 2A). They were negative for Tuj-1, a neuron-specific tubulin, and neurofilament M (NF-M) (Figs. 2B, C).

2.2. *Effects of "chemical induction" on morphology and immunocytochemistry*

To induce "neuronal differentiation" of the BMSC chemically, the BMSC were treated with the induction medium containing DMSO, bFGF, and RA on fibronectin coated 4-well culture slides or 75-cm^2 flasks. After exposure to the induction medium, the polygonal BMSC with flat cytoplasm began to retract, and the cell body became compact within 1 h (Fig. 1B). Simultaneously, a small part of the BMSC detached from the culture slide and floated in the medium. The adherent cells were kept incubated with the induction medium. At days 5–6, a part of the cells showed spherical cell body with bipolar or multi-polar processes that appeared to be connecting to each other (Figs. 1C, D). There still existed the cells that retained their original morphology (Fig. 1D). Similar morphological changes were reproducible in triplicate experiments.

We next evaluated the effect of "chemical induction" on the expression of the neuronal markers nestin, Tuj-1, and NF-M. After exposure to DMSO, bFGF, and RA, approximately 56% of the cells showed immunoreactivity against nestin (Fig. 2D), and 18% of the cells showed positive staining for Tuj-1 (Fig. 2E). On the other hand, immunoreactivity against NF-M was not detected (Fig. 2F). Therefore, "chemical induction" significantly amplified the immunoreactivity against nestin and Tuj-1.

2.3. *Gene expression profile of the BMSC*

Of 251 genes identified in human BMSC by Seshi et al. (2003), 115 genes could be identified in the mice BMSC on microarray analysis (Table 1). Their normalized signal intensities ranged from 0.4 to 527.1. These 115 identified genes could be classified into 10 derivative groups: 9 osteoblast-associated, 15 muscle/muscle disorders-associated, 8 fibroblast-associated, 3 adipocyte-associated, 11 epithelial cell/carcinoma-associated, 6 endothelial cell-associated, 35 nerve cell/neuroendocrine/neurologic disorders-associated, 7 myeloid cell/myeloid leukemia-associated, 4 T cell/NK cell-associated, and 17 B cell/B cell neoplasm-associated genes (Table 1).

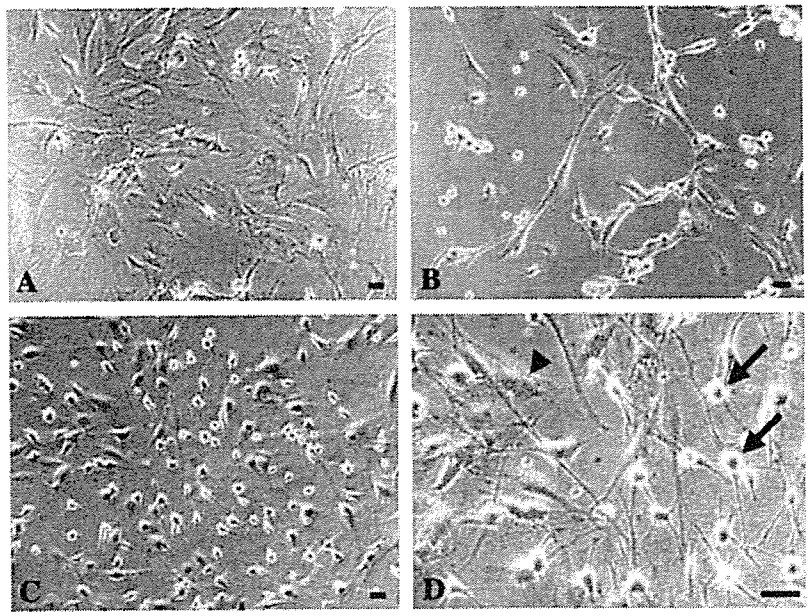

Fig. 1 – Microphotographs of the marrow stromal cells (MSCs) before and after "chemical induction". (A) The MSCs from P3 demonstrated a flat and polygonal appearance. (B) After exposure to induction medium, MSCs began to retract, and the cell body became compact within 1 h. (C), (D) At days 5–6, a portion of the cells developed a spherical cell body with bipolar or multi-polar processes that appeared to be connecting each other (arrows). There still existed the cells that retained their original morphology (arrowhead). Scale bar = 50 μm.

Of the 10 genes showing the highest normalized signal intensities, 4 were muscle-associated genes including actin (Acta2, NM_007392.2), capping protein (Capzb, NM_009798.1), transgelin (Tagln, NM_011526.2), and tropomyosin 1 (Tpm1, NM_024427.2); 3 were osteoblast-associated genes, including biglycan (Bgn, NM_007542.3), procollagen (Col1a2, NM_007743.1), and secreted acidic cysteine rich glycoprotein (Sparc, NM_009242.1); 2 were nerve cell/neuroendocrine/neurologic disorder-associated genes, including diazepam binding inhibitor (Dbi, NM_007830.2) and neural precursor cell expressed, developmentally down-regulated gene 8 (Nedd8, NM_008683.1); 1 was an epithelial cell-associated gene, thymosin beta 4x chromosome (Tmsb4x, NM_021278.1). Their normalized signal intensities ranged from 81.7 to 527.1.

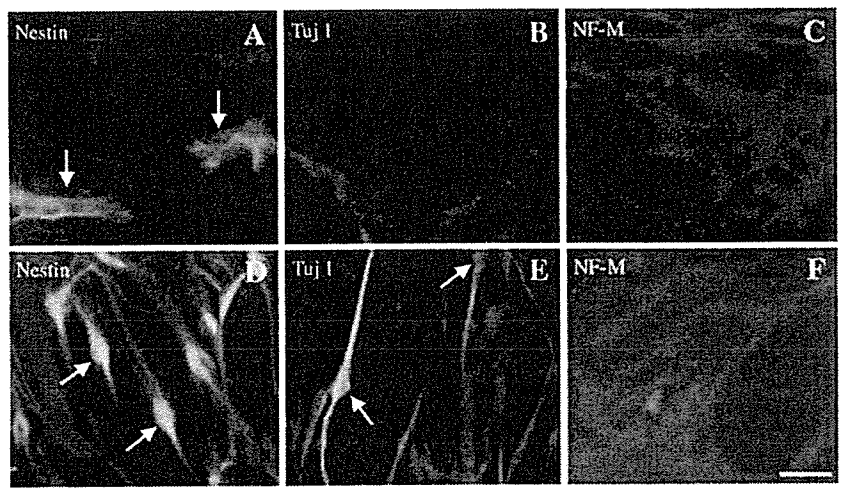

Fig. 2 – Immunocytochemistry of the marrow stromal cells (MSCs) before (upper panels) and after (lower panels) "chemical induction". The MSCs were stained with primary antibodies against nestin (A and D), Tuj 1 (B and E), and neurofilament M (C and F). (A) Approximately 8% of the untreated MSCs were positive for nestin (arrows). (B), (C) The MSCs were negative for Tuj 1 and neurofilament M (NF-M). (D), (E) After "chemical induction", approximately 56% of the cells showed immunoreactivity against nestin, and 18% of the cells showed positive staining for Tuj 1 (arrows). (F) Immunoreactivity against NF-M was not detected (Fig. 2F). Scale bar = 50 μm.

Table 1 – List of 115 genes of mouse bone marrow stromal cells detected by microarray analysis and the alteration of their expression after "chemical induction"

Cellular lineage (number of genes)	Gene title	Symbol	Accession #	Normalized signal intensity		Ratio	Outcome
				Untreated MSC	Treated MSC		
Osteoblast/ Bone cell/ bone disorder-associated genes (9)	Basic helix–loop–helix domain-containing, class B2	Bhlhb2	NM_011498.2	3.885020614	8.713078963	2.242736868	Increased
	Biglycan	Bgn	NM_007542.3	90.4212594	5.317904509	−17.0031747	Decreased
	Cadherin 11	Cdh11	NM_009866.2	5.182928189	0.779358572	−6.650248515	Decreased
	Chondroitin sulfate proteoglycan 2	Cspg2	NM_019389.1	24.8950116	1.627993462	−15.29183757	Decreased
	Chondroitin sulfate preteoglycan 6	Cspg6	NM_007790.1	0.619477951	0.414669588	−1.493907362	N.S.
	Procollagen, type I, alpha 2	Col1a2	NM_007743.1	137.2792468	9.058491585	−15.15475789	Decreased
	Exostoses (multiple) 1	Ext1	NM_010162.1	34.96779024	30.9316686	−1.130485092	N.S.
	Secreted acidic cysteine rich glycoprotein	Sparc	NM_009242.1	409.5148505	81.24491285	−5.040498367	Decreased
	Vitamin D receptor	Vdr	NM_009504.2	0.672225429	0.467615143	−1.43756129	N.S.
Muscle/muscle disorders-associated genes (15)	Actin, alpha2, smooth muscle, aorta	Acta2	NM_007392.2	527.1075523	7.549197721	−69.82298938	Decreased
	Beclin 1 (coiled-coil, myosin-like bcl2-interacting protein)	Becn1	NM_019584.2	19.47121572	18.49113734	−1.053002601	N.S.
	Caldesmon 1	Cald1	NM_145575.1	14.71938823	4.660527501	−3.15830949	Decreased
	Capping protein (actin filament) muscle Z-line, alpha 2	Capza2	NM_007604.1	22.02270606	24.77897117	1.125155606	N.S.
	Capping protein (actin filament) muscle Z-line, beta	Capzb	NM_009798.1	104.6202909	87.48084592	−1.19592226	N.S.
	Cytochrome C oxidase, subunit VII a 1	Cox7a1	NM_009944.2	1.492803544	4.712045049	3.156507142	Increased
	FSHD region gene 1	Frg1	NM_013522.1	11.66722116	12.19467838	1.045208471	N.S.
	Fukuyama type congenital muscular dystrophy homolog (human)	Fcmd	NM_139309.2	3.870947041	4.858913008	1.255225906	N.S.
	Muscle bind-like (DROSOPHILIA)	Mbnl	NM_020007.1	3.410656694	4.013118734	1.176641068	N.S.
	Myosin IB	Myo1b	NM_010863.1	7.54103479	2.905599124	−2.595345906	Decreased
	Myosin X	Myo10	NM_019472.1	1.75355016	0.783559244	−2.237929263	Decreased
	Pyruvate kinase, muscle	Pkm2	NM_011099.2	32.24850751	46.60788329	1.445272569	N.S.
	Transgelin	Tagln	NM_011526.2	144.3332086	3.283673618	−43.95479738	Decreased
	Tropomyosin 1	Tpm1	NM_024427.2	82.89211777	4.862828877	−17.04606925	Decreased
	Tropomyosin 2, beta	Tpm2	NM_009416.2	4.968675576	3.789955791	−1.311011487	N.S.
Fibroblast-associated genes (8)	Fibrillin 1	Fbn1	NM_007993.1	74.57276666	7.929973475	−9.403911236	Decreased
	Fibroblast activation protein	Fap	NM_007986.1	0.826438448	0.805993566	−1.025366061	N.S.
	Fibroblast growth factor 7	Fgf7	NM_008008.2	7.891960303	2.921189553	−2.70162554	Decreased
	Fibroblast growth factor receptor 1	Fgfr1	NM_010206.1	2.146773158	3.940144683	1.835380076	N.S.
	Alpha-1 type IV collagen	Col4a1	J04694.1	13.71690236	5.945904197	−2.306949776	Decreased
	Prolyl 4-hydroxylase alpha(I)-subunit	P4ha1	U16162.1	8.800490633	13.16640866	1.496099389	N.S.
	Procollagen-proline, 2-oxoglutarate 4-dioxygenase (proline4-hydroxylase), alpha II polypeptide	P4ha2	NM_011031.1	1.575733041	1.459224561	−1.079842735	N.S.
	Syndecan 2	Sdc2	NM_008304.1	18.56375235	7.69932045	−2.411089715	Decreased
Adipocyte-associated genes (3)	Degenerative spermatocyte homolog (*Drosophila*)	Degs	NM_007853.2	53.22277499	87.11530576	1.636805029	N.S.
	High density lipoprotein (HDL) binding protein	Hdlbp	NM_133808.2	72.27156158	64.2940847	−1.124077929	N.S.
	Necdin	Ndn	NM_010882.2	21.5069733	12.45538748	−1.726720532	N.S.
Epithelial cell/ carcinoma-associated genes (11)	Ectodermal-neural cortex 1	Enc1	NM_007930.2	0.411996988	0.464511851	1.12746419	N.S.
	Epidermal growth factor receptor pathway substrate 15	Eps15	NM_007943.1	1.663247101	1.847638065	1.110862039	N.S.
	Epidermal growth factor receptor pathway substrate8	Eps8	NM_007945.1	14.08394031	24.36495832	1.729981652	N.S.
	Mad homolog 4 (*Drosophila*)	Madh4	NM_008540.2	1.289772672	1.187321724	−1.086287436	N.S.

Table 1 (*continued*)

Cellular lineage (number of genes)	Gene title	Symbol	Accession #	Normalized signal intensity		Ratio	Outcome
				Untreated MSC	Treated MSC		
	Milk fat globule-EGF factor 8 protein	Mfge8	NM_008594.1	29.06378591	32.59474069	1.121489843	N.S.
	Prothymosin alpha	Ptma	NM_008972.1	67.53634544	52.35996645	−1.289846996	N.S.
	Epithelial membrane protein 1	Emp1	NM_010128.3	0.958770664	0.63322884	−1.514098228	N.S.
	Polymeric immunoglobulin receptor	Pigr	NM_011082.2	1.472519837	0.476139378	−3.092623515	Decreased
	Breast cancer anti-estrogen resistance 3	Bcar3	NM_013867.1	13.65853192	3.476749548	−3.928534896	Decreased
	Lectin, galactose binding, soluble 8	Lgals8	NM_018886.2	4.943197435	4.373541114	−1.130250592	N.S.
	Thymosin, beta 4, X chromosome	Tmsb4x	NM_021278.1	428.4805665	414.2536076	−1.034343597	N.S.
Endothelial cell-associated genes (6)	Tumor necrosis factor, alpha-induced protein 1 (endothelial)	Tnfaip1	NM_009395.2	7.503479037	3.837293934	−1.955408985	N.S.
	Vascular endothelial growth factor C	Vegfc	NM_009506.1	1.352103776	0.68573723	−1.971752031	N.S.
	Endothelial differential, lysophosphatidic acidic G-protein-coupled receptor, 2	Edg2	NM_010336.1	9.762849105	10.3008077	1.055102624	N.S.
	Vascular cell adhesion molecule 1	Vcam1	NM_011693.2	2.163260219	2.103464683	−1.028427164	N.S.
	Vascular endothelial growth factor B	Vegfb	NM_011697.1	5.101605709	5.794002608	1.135721367	N.S.
	Endothelial differentiation-related factor 1	Edf1	NM_021519.1	55.12837019	76.34880278	1.384927625	N.S.
Nerve cell/ neuroendocrine/ neurologic disorders-associated genes (35)	Amyloid beta (A4) precursor protein	App	NM_007471.1	2.487359408	2.076818081	−1.19767804	N.S.
	Brain derived neurotropic factor	Bdnf	NM_007540.3	15.07925447	18.19569494	1.206670726	N.S.
	Cadherin 2	Cdh2	NM_007664.1	2.548244892	1.620131806	−1.572862704	N.S.
	Cerebellar degeneration-related 2	Cdr2	NM_007672.1	7.536403578	5.039725992	−1.49539947	N.S.
	Diazepam binding inhibitor	Dbi	NM_007830.2	112.9080406	81.54587454	−1.384595373	N.S.
	Glioblastoma amplified sequence	Gbas	NM_008095.1	3.391257806	3.141684493	−1.079439331	N.S.
	Neuroblastoma, suppression of tumorigenicity 1	Nbl1	NM_008675.1	10.39337676	5.54481151	−1.874432836	N.S.
	Neural precursor cell-expressed, developmentally down-regulated gene 8	Nedd8	NM_008683.1	81.7276398	99.0781461	1.212296676	N.S.
	Peripheral myelin protein 22	Pmp22	NM_008885.1	68.92661086	115.1324124	1.670362302	N.S.
	Presenilin 1	Psen1	NM_008943.1	4.754547162	9.001027502	1.89314086	N.S.
	Spinocerebellar ataxia 1 homolog (human)	Sca1	NM_009124.1	5.0941124	3.5446538	−1.43712551	N.S.
	Spinocerebellar ataxia 2 homolog (human)	Sca2	NM_009125.1	1.451159679	1.462697033	1.007950438	N.S.
	Serine palmitoyl tansferase, long chain base subunit 1	Sptlc1	NM_009269.2	3.735772543	6.010424661	1.608883997	N.S.
	Adrenomedullin	Adm	NM_009627.1	18.02575009	45.32395831	2.514400681	Increased
	Activity-dependent neuroprotective protein	Adnp	NM_009628.1	0.548876291	0.460056709	−1.193062248	N.S.
	Ankyrin 3, epithelial, transcript variant 7	Ank3	NM_009670.2	3.72620285	0.757209349	−4.920967834	Decreased
	Ceroid-lipofuscinosis, neuronal 2	Cln2	NM_009906.2	41.27851806	87.01538462	2.108006505	Increased
	Lim domain only 4	Lmo4	NM_010723.2	14.41241487	6.546405611	−2.201576824	Decreased
	Max interacting protein 1	Mxi1	NM_010847.1	1.551743726	2.591191722	1.66985803	N.S.
	Ubiquitin carboxy-terminal hydroxylase L1	Uchl1	NM_011670.1	14.26599627	4.948926935	−2.88264435	Decreased
	Enolase 2, gamma neuronal	Eno2	NM_013509.2	1.417623773	3.84822081	2.714557192	Increased
	Zinc finger homeobox 1B	Zfhx1b	NM_015753.1	0.445082516	0.635664336	1.428194354	N.S.
	Huntingtin interacting protein 2	Hip2	NM_016786.2	76.82446946	90.68386623	1.180403417	N.S.
	Spinocerebellar ataxia 10 homolog (human)	Sca10	NM_016843.1	31.11847325	24.42464803	−1.274060253	N.S.

(continued on next page)

Table 1 (*continued*)

Cellular lineage (number of genes)	Gene title	Symbol	Accession #	Normalized signal intensity		Ratio	Outcome
				Untreated MSC	Treated MSC		
	Prostaglandin D2 synthase 2, hematopoietic	Ptgds2	NM_019455.2	2.567587917	11.38198896	4.432950038	Increased
	Gamma-aminobutyric acid receptor-associated protein	Gabarap	NM_019749.2	81.17417744	81.453687	1.003443331	N.S.
	Axotrophin	Axot	NM_020575.1	1.677082962	2.463219217	1.468752157	N.S.
	Gamma-aminobutyric acid (GABA (A)) receptor-associated protein-like 1	Gabarapl1	NM_020590.3	0.923792532	1.502479339	1.626425075	N.S.
	Glia maturation factor, beta	Gmfb	NM_022023.1	19.42065427	34.51289837	1.77712336	N.S.
	Stathmin-like 2	Stmn2	NM_025285.1	12.02988769	1.870078535	−6.432824858	Decreased
	GABA(A) receptor-associated protein like 2	Gabarapl2	NM_026693.2	31.1907534	66.22951975	2.123370311	Increased
	Neural precursor cell-expressed, developmentally down-regulated gene 4-like	Nedd4l	NM_031881.1	5.250100988	3.685830239	−1.424401193	N.S.
	Amyloid beta precursor protein binding protein 1	Appbp1	NM_144931.1	18.36765723	18.97146646	1.032873503	N.S.
	Was protein family, member 3	Wasf3	NM_145155.1	2.536669756	2.367429848	−1.071486768	N.S.
	Brain glycogen phosphorylase	Pygb	NM_153781.1	7.976188842	7.886438992	−1.011380276	N.S.
Myeloid cell/myeloid leukemia-associated genes (7)	Testis-specific c-abl protein	Abl1	J02995.1	11.56376983	9.892374005	−1.16895801	N.S.
	Myeloid cell leukemia sequence 1	Mcl1	NM_008562.2	9.098262421	15.40934035	1.693657496	N.S.
	Runt related transcription factor 1	Runx1	NM_009821.1	2.013017043	1.873896362	−1.074241395	N.S.
	Core binding factor beta	Cbfb	NM_022309.2	16.84739337	15.98339735	−1.054055843	N.S.
	Set translocation	Set	NM_023871.2	35.033014	29.01666628	−1.207341108	N.S.
	Homolog of human Mlt2 unidentified gene	Mllt2h	NM_133919.2	6.120160571	5.035593814	−1.215380111	N.S.
	Phosphatidylinositol binding clathrin assembly protein	Picalm	NM_146194.2	38.86745857	56.13559127	1.444282527	N.S.
T cell/NK cell-associated genes (4)	RAP1, GTP-GDP dissociation stimulator 1	Rap1gds1	NM_145544.1	21.67508296	31.04415459	1.432250785	N.S.
	Natural killer tumor recognition sequence	Nktr	NM_010918.1	9.161865846	9.790960546	1.068664474	N.S.
	CD4 antigen	Cd4	NM_013488.1	1.626727316	1.895045293	1.164943427	N.S.
	Transcription elongation regulator 1	Tcerg1	NM_019512.1	3.832580223	3.722356238	−1.029611348	N.S.
B cell/B cell neoplasm-associated genes (17)	Core promoter binding protein	Copeb	AF072403.1	13.13153365	11.05024565	−1.188347668	N.S.
	B lymphoma MO-MLV insertion region 1	Bmi1	NM_007552.1	0.951603663	0.635055462	−1.498457569	N.S.
	Zinc finger protein 36, C3H type-like 1	Zfp36l1	NM_007564.1	5.593461634	5.523224768	−1.012716641	N.S.
	Cyclin D1	Ccnd1	NM_007631.1	6.419276267	13.2491743	2.063966987	Increased
	Nuclear factor of kappa light chain gene enhancer in B cells 1	Nfkb1	NM_008689.1	4.424448353	5.136184375	1.160864353	N.S.
	V-rel reticuloendotheliosis viral oncogene homolog A	Rela	NM_009045.2	2.422276539	1.95526373	−1.238849011	N.S.
	Transcription factor 3	Tcf3	NM_009332.1	0.556868867	0.563828389	1.012497596	N.S.
	B cell leukemia/lymphoma 6	Bcl6	NM_009744.2	1.900417417	1.675891541	−1.133973989	N.S.
	General transcription factor II I	Gtf2i	NM_010365.1	22.59905643	20.07810345	−1.125557326	N.S.
	Nuclear factor of kappa light chain gene enhancer in B cells inhibitor, alpha	Nfkbia	NM_010907.1	20.81323338	45.53106592	2.187601758	Increased
	Tumor necrosis factor receptor superfamily, member 5	Tnfrsf5	NM_011611.1	0.793886537	0.81256175	1.023523781	N.S.
	Pre B cell leukemia transcription factor 3	Pbx3	NM_016768.1	0.918218046	0.60364539	−1.521121609	N.S.
	Reed-Steinberg cell-expressed intermediate filament-associated protein (restin)	Rsn	NM_019765.2	3.333170862	2.60403183	−1.280003886	N.S.
	General transcription factor II I repeat domain-containing 1	Gtf2ird1	NM_020331.1	10.04378892	7.196487343	−1.395651579	N.S.
	V-RAL simian leukemia viral oncogene homolog B (RAS related)	Ralb	NM_022327.3	1.492763916	0.8463347	−1.763798549	N.S.
	V-RAF-1 leukemia viral oncogene1	Raf1	NM_029780.1	8.040491641	8.987247019	1.117748444	N.S.
	Protein-tyrosine-phosphatase	Ptprf	Z23061.1	1.53457988	1.103643404	−1.390467133	N.S.

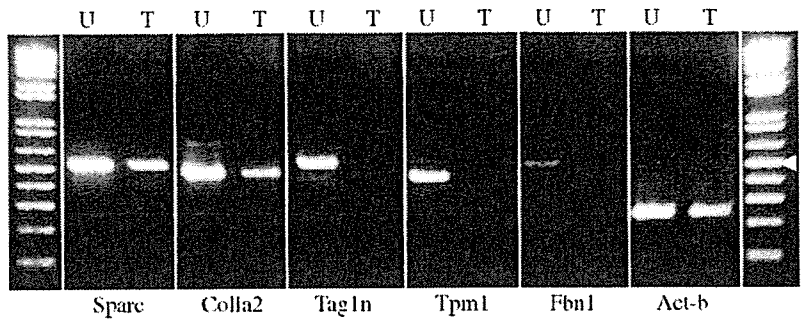

Fig. 3 – Expression of the neuronal markers before and after "chemical induction" as evaluated by RT-PCR. Definite expression of nestin and Tuj 1 and faint expression of NF-M was detected on RT-PCR in both untreated (U) and treated MSCs (T). (kb: 1-kb DNA ladder, Arrow head: 500-bp DNA fragment).

The results indicated that the BMSC per se express multilineage cellular genes.

We then evaluated the gene expression profile of 3 neuronal markers—nestin, Tuj-1, and NF-M—in the BMSC because these genes were not included in the abovementioned 115 genes. As a result, their genes were expressed with rather low normalized signal intensities. The values for nestin, Tuj-1, and NF-M were 5.4, 2.9, and 0.8, respectively. These results correlated very well with the finding that the percentage of BMSC positive for these markers was very low on immunocytochemistry.

2.4. *Effects of "chemical induction" on gene expression profile in the BMSC*

As the next step, we evaluated the effects of treatment with DMSO, bFGF, and RA on the gene expression profile in the BMSC. As shown in Table 1, "chemical induction" significantly altered the expression profile in 30 out of the 115 genes identified in the BMSC. Normalized signal intensity markedly decreased to lower than 10% of the control value in 5 out of 9 osteoblast-associated genes, including the genes for biglycan (Bgn, NM_007542.3) and procollagen (Colla2, NM_007743.1). Similar findings were also observed in 6 out of 15 muscle-associated genes. In particular, the gene for actin (Acta2, NM_007392.2) reduced the normalized signal intensity from 527.1 to 7.5 (1.4%) after "chemical induction". The normalized signal intensity also decreased in 4 out of 8 fibroblast-associated genes, for example, from 74.6 to 7.9 (10.6%) in the gene for fibrillin 1 (Fbn1, NM_007993.1). On the other hand, only two of 32 osteoblast-, muscle-, and fibroblast-associated genes showed significant, but mild, increases in normalized signal intensity. Therefore, the microarray analysis showed that "chemical induction" with DMSO, bFGF, and RA dramatically reduced the expression of the genes related to the mesodermal derivatives. RT-PCR analysis also verified that "chemical induction" reduced the expression of the genes for Acta2 (NM_007392.2), Tagln (NM_011526.2), Tpm1 (NM_024427.2), Bgn (NM_007542.3), chondroitin sulfate proteoglycan 2 (Cspg2, NM_019389.1) and Col1a2 (NM_007743.1), all of which were associated with the osteoblast/bone cell/bone disorder and muscle/muscle disorder sublists (Fig. 3).

"Chemical induction" significantly altered the normalized signal intensity in 9 out of 35 genes associated with nerve cell/neuroendocrine/neurologic disorder. A significant decrease was identified in 4 genes, including ankyrin 3 (Ank3, NM_009670.2), lim domain only 4 (Lmo4, NM_010723.2), ubiquitin carboxy-terminal hydroxylase L1 (Uchl1, NM_011670.1), and stathmin-like 2 (Stmn2, NM_025285.1). Their original normalized signal intensity was relatively low, ranging from 3.7 to 14.4, and further decreased after "chemical induction". On the other hands, the normalized signal intensity significantly increased in 5 genes, including adrenomedullin (Adm, NM_009627.1), ceroid-lipofuscinosis (Cln2, NM_009906.2), enolase 2 (Eno2, NM_013509.2), prostaglandin D2 synthase 2 (Ptgds2, NM_019455.2), and GABA(A) receptor-associated protein like 2 (Gabarapl2, NM_026693.2). Their original values ranged from 1.4 to 41.3 and increased to 3.8 to 87.0 after "chemical induction" (Table 1).

In the present study, "chemical induction" significantly altered the normalized signal intensity in only a few gene related to other derivatives (Table 1).

Finally, we assessed the alteration of expressions of genes for nestin, Tuj-1, and NF-M after "chemical induction" and found no significant modifications of their normalized signal intensity. RT-PCR analysis confirmed these results (Fig. 4).

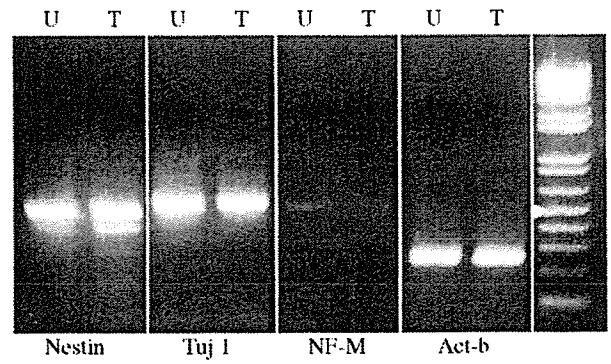

Fig. 4 – Alteration of specific gene expression in the marrow stromal cells (MSCs) after "chemical induction" detected by semiquantitative RT-PCR. When compared with the untreated MSCs (U), expression of osteoblast-associated (Sparc, Col1a2), muscle-associated (Tagln, Tpm1), and fibroblast-associated (Fbn1) genes decreased in the treated MSCs (T). Act-b was used as an internal control. (kb: 1-kb DNA ladder, arrowhead: 500-bp DNA fragment).

2.5. *Gene expression of neurotrophic/neuroprotective factors in BMSC*

To clarify whether the BMSC constitutively express the genes for neurotrophic or neuroprotective factors, we evaluated their normalized signal intensity on microarray analysis. Microarray analysis revealed that the untreated BMCS expressed the genes for 7 cytokines or growth factors known to have neurotrophic or neuroprotective effects. They included nerve growth factor-beta (NGFb, NM_013609.1), ciliary neurotrophic factor (CNTF, NM_053007.1), glia maturation factor-beta (Gmfb, NM_022023.1), brain derived neurotrophic factor (BDNF, NM_007540.3), interleukin 6 (IL6, NM_031168.1), insulin-like growth factor 1 (IGF1, NM_010512.2), and transforming growth factor-beta 3 (TGFb3, NM_009368.1). Their normalized signal intensities ranged from 5.3 to 28.3. Qualitative RT-PCR analysis was also performed to verify the results on microarray analysis. As shown in Fig. 5, RT-PCR analysis indicated that the untreated BMSC expressed mRNA for the 7 factors, although mRNA for BDNF was only faintly expressed.

Lastly, the effects of "chemical induction" on the expression profiles of the genes for these factors were evaluated using microarray analysis. "Chemical induction" reduced the normalized signal intensities for NGFb (12.9 to 5.4), CNTF (5.3 to 0.9), IL6 (15.8 to 0.7), and TGFb3 (28.3 to 4.8), while it increased the normalized signal intensity for Gmfb (19.4 to 34.5). No significant changes were observed in the normalized signal intensities for BDNF (15.1 to 18.2) and IGF1 (12.6 to 14.2).

3. Discussion

The present study demonstrates that the BMSC express multilineage cellular genes as previously reported, but that the morphological, immunostaining, and microarray analysis of the BMSC after in vitro chemical treatments could not directly prove their capacity for neuronal differentiation. On the other hand, the chemical treatment in this study significantly altered BMSC gene expression profiles for several cellular lineages. The BMSC dramatically reduced the expression of genes for the mesenchymal cell lineages and partly expanded the expression of genes associated with neurons. These findings strongly suggest that at least a certain subpopulation of the BMSC have multipotency and can alter their gene expression profile in response to the surrounding environment. The present study also revealed that the BMSC expressed mRNA for various kinds of neurotrophic or neuroprotective factors.

3.1. *Gene expression profile changes in BMSC during in vitro treatment*

Several chemical agents have previously been reported to promote the BMSC to differentiate into neurons. Sanchez-Ramos et al. (2000) cultured human BMSC in the presence of epidermal growth factor (EGF) or brain-derived neurotrophic factor (BDNF) and RA, and they reported that a minor population of the BMSC expressed nestin, GFAP, and neuron-specific nuclear protein (NeuN) (Sanchez-Ramos et al., 2000). Woodbury et al. (2000) also cultured rat BMSC with bFGF and then with agents including dimethylsulfoxide (DMSO), β-mercaptoethanol (BME), and butylated hydroxyanisole (BHA). They found that the BMSC showed a rapid morphological change mimicking that of neurons, and that they expressed specific neuronal markers, including nestin, NSE, NeuN, NF-M, tau, and trkA (Woodbury et al., 2000). Kohyama et al. (2001) treated the BMSC with 5-azacytidine to alter the gene expression pattern and cultured the BMSC with NGF, BDNF, and neurotrophin 3, reporting similar results (Kohyama et al., 2001). Exposure of the BMCS to dibutyryl cyclic AMP (dbcAMP) and isobutylmethylxanthine (IBMX) has also been reported to promote their differentiation into neurons (Deng et al., 2001). Overall, the chemical treatment protocols with these agents have obtained the following results: (1) treated BMSC rapidly expressed neuronal phenotype within several hours; (2) at most, 80% of the cells expressed the neuronal markers NSE and NF-M; (3) stem cells derived from the muscle and adipose tissue also expressed the neuronal phenotype via this protocol (Romero-Ramos et al., 2002; Safford et al., 2002; Woodbury et al., 2000, 2002).

Furthermore, the extracellular matrix may be an important environmental factor for BMSC differentiation. Thus, Kim et al. (2002) treated BMSC with RA and bFGF on dishes coated with different substrates: laminin, gelatin, collagen, poly-ornithine, and fibronectin. Expression of neuronal phenotypes was most prominent when BMSC were cultured on fibronectin, a substrate that is known to promote neurite outgrowth (Kim et al., 2002).

However, recent experiments have raised questions concerning these previous results. Rismanchi et al. (2003)

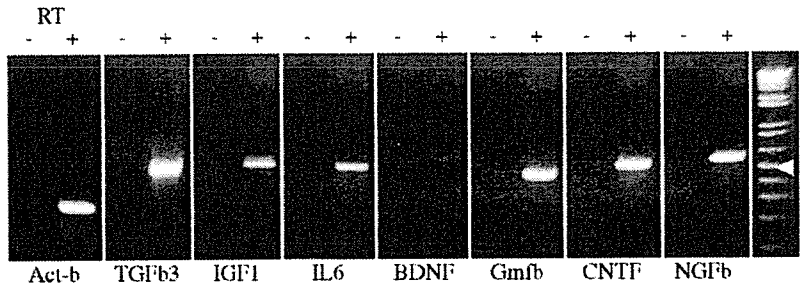

Fig. 5 – Expression of the genes for 7 cytokines or growth factors as detected by RT-PCR. +Reverse transcriptase was added to the reaction, –negative control without reverse transcriptase. Expression of NGFb, CNTF, Gmfb, IL6, IGF1, and TGFb was confirmed. BDNF yielded a faint single band. Arrowhead, 500-bp DNA fragment.

reported that the treatment of the BMSC with agents including DMSO yields a high percentage of cell death, indicating that a non-physiological condition caused by exposure to DMSO might result in the cell death (Rismanchi et al., 2003). Furthermore, as described in the introduction, careful morphological analysis and RT-PCR technique strongly indicated that BMSC in vitro neuronal differentiation might be an artifact of exposure to the chemical agents (Lu et al., 2004; Neuhuber et al., 2004).

Based on these considerations, we cultured the BMSC with medium containing DMSO, bFGF and RA and evaluated the changes in their morphology and phenotype as the first step of the experiment. Our protocol yielded a morphological change similar to the abovementioned studies (Deng et al., 2001; Woodbury et al., 2000, 2002). Immunocytochemistry also indicated increased immunoreactivity against nestin and Tuj-1. The results suggested that the chemical treatment might induce BMSC differentiation into immature neurons. However, microarray and RT-PCR analyses showed no significant change in the normalized signal intensity of the genes for nestin and Tuj-1. As pointed out before, the immunocytochemical findings may result from cellular shrinkage (Lu et al., 2004; Neuhuber et al., 2004). Therefore, the results do not support BMSC potential to differentiate into neurons, at least when treated with DMSO, bFGF and RA in vitro. As Neuhuber et al. (2004) also pointed out (Neuhuber et al., 2004), however, the results never deny the multipotency of the BMSC itself. Thus, the analysis of only specific genes for nestin, Tuj-1, and NF-M may be incomplete to reject this notion because numerous genes have been identified in the BMSC, only a portion of which are related to neural cells. For example, Tremain et al. (2001) reported that mouse and human BMSC simultaneously expressed the genes related to various mesenchymal cell lineages including chodrocytes, myoblasts, osteoblasts, and the endothelial, epithelial, and neuronal cell lineages (Seshi et al., 2003; Tremain et al., 2001; Wieczorek et al., 2003; Woodbury et al., 2002).

Therefore, we considered it essential to precisely dissect the effects of chemical treatment on the expression profile of genes for multiple cellular lineages in the BMSC. First, in this preliminary report, we analyzed the effects of chemical treatment on the expression profile primarily of the 115 genes previously identified in the human BMSC. Microarray and RT-PCR analyses revealed that treatment with DMSO, bFGF, and RA dramatically reduced the expression of the genes associated with mesodermal derivatives such as bone and muscle (Table 1, Fig. 3). On the other hands, 5 out of 35 genes related to neural cells significantly increased their normalized signal intensity after the treatment (Table 2). Although the treatment protocol in this study did not induce the BMSC to totally differentiate into the neuron, the results strongly suggest that BMSC are ready to alter their gene expression profile and to diminish their characteristics as mesenchymal cells after exposure to DMSO, bFGF, and RA. Similar findings have been reported by Woodbury et al. (2002). Using the RT-PCR technique, they showed that chemical treatment with DMSO and BHA decreased the expression of ceruloplasin and protamine2 and that NF-M and tau increased with ongoing neuronal differentiation (Woodbury et al., 2002). To our best knowledge, however, there is no report that denoted the change in gene expression profile of the BMSC after chemical treatment using microarray analysis. The present finding that BMSC can alter their gene expression profile in response to the surrounding environment within several days should be noted when studying the role and underlying mechanism of BMSC transplantation therapy. Very recently, Egusa et al. (2005) reported similar results and speculated that decreased microarray signals in the induced BMSC might result from silencing of superfluous gene clusters (Egusa et al., 2005).

3.2. *Limitations of this study*

There are certain limitations to this study which should be noted. In this preliminary report, we primarily analyzed the 115 genes that have been identified in human BMSC by Seshi et al. (2003) (Seshi et al., 2003). Therefore, we do not define the behavior of numerous other genes in response to the in vitro differentiation protocol. Further study would be necessary to analyze the changes in each of the 20,000 genes identified by microarray analysis, characterizing the effects of chemical treatment more precisely. As described above, we extracted the RNA from cultured cells that adhered to the flask bottom. Consequently, microarray analysis data in this study are not based on the cells expanded from a single cell but represent the sum total of gene expression profile in the heterogeneous population of the BMSC. Thus, there is the possibility that the results may be diluted even if the cultured cells include the subpopulation of cells with strong neurogenic potential. We also cannot deny the possibility that the results may be influenced by the loss of some cell populations. Furthermore, as described above, previous reports have shown that a certain subpopulation of the BMSC survive without evidence of rejection or inflammation, migrate towards the lesion, morphologically mimic the neuron, and express proteins specific for the neuron when transplanted into animal models of various neurological disorders (Chen et al., 2002a; Chopp et al., 2000; Kopen et al., 1999; Lee et al., 2003, 2004; Mahmood et al., 2001; Ohta et al., 2004; Shichinohe et al., 2004; Wu et al., 2003). However, based on the present results, we cannot reach the conclusion that the transplanted BMSC do not differentiate into neural cells because the in vivo environment in the injured CNS would be quite different from the in vitro conditions of this study (Rismanchi et al., 2003). Therefore, it is necessary to investigate the behavior of the BMSC from a different point of view when the untreated BMSC are transplanted into the injured CNS as cell replacement therapy. Furthermore, it should be remembered that the period of in vitro experimentation in this study may be too short to mimic the entirety of behaviors of BMSC transplanted into the CNS and that "chemical induction" itself may be quite different for the BMSC in the CNS.

The present study focused on the gene expression profile in BMSC transplanted into the CNS. Of course, a functional assay is essential to discuss how the transplanted BMSC contribute to functional recovery. Using autoradiography and immunocytochemistry, we have recently shown that the BMSC express the gamma-aminobutyric acid (GABA) receptor and a specific neuronal marker, MAP2, in the peri-infarct neocortex when transplanted into mice with cerebral infarct, suggesting that

the transplanted BMSC may contribute to the improved receptor function around cerebral infarct (Shichinohe et al., in press).

3.3. *Expression of genes for growth factors in BMSC*

Because BMSC play an important role in the maturation and differentiation of hematopoietic stem cells through cell–cell interactions in the bone marrow (Deans and Moseley, 2000), it is not surprising that they secrete various cytokines or growth factors that promote hematopoiesis. Chen et al. (2002a,b) reported that BMSC increased their production of BDNF, NGF, vascular endothelial growth factor (VEGF), and hepatocyte growth factor (HGF) when cultured in the supernatant from ischemic or traumatic brain tissue extracts (Chen et al., 2002b). Some investigators have attributed the beneficial effects of BMSC transplantation therapy to their secretion of trophic or protective factors (Chen et al., 2002b; Lou et al., 2003; Ohta et al., 2004). The present results indicated that BMSC spontaneously express mRNA for several neurotrophic/neuroprotective factors, including NGFb, CNTF, Gmfb, BDNF, IL6, IGF1, and TGFb3, partially correlating with previous reports (Garcia et al., 2004; Tremain et al., 2001; Wieczorek et al., 2003). However, "chemical induction" did not increase the normalized signal intensities for these factors, with the exception of Gmfb. Although the present study was constrained to assess gene expression at transcription level, a cocktail of neurotrophic/neuroprotective factors derived from the BMSC may have therapeutic effects in the damaged CNS. At the very least, the "chemical induction" protocol in this study did not enhance the expression of genes for most of these factors.

In conclusion, microarray and RT-PCR analyses indicated that the morphological change and expression of specific neuronal proteins in the BMSC after "chemical induction" were not directly linked to their neuronal differentiation. However, chemical treatment no doubt altered their gene expression profile for several cellular lineages. Thus, BMSC have the potential to alter their gene expression profile in response to the surrounding environment. The neurogenic potential of the BMSC should be further studied to clarify the underlying mechanism of the therapeutic effects of BMSC transplantation into the injured CNS. The present study also demonstrated that BMSC express mRNA for various kinds of neurotrophic or neuroprotective factors, supporting the theory that BMSC improve neurological functions, at least in part, by interacting with host neural cells.

4. Experimental procedures

4.1. *Isolation of mice bone marrow stromal cells*

All animal experiments were approved by the Animal Studies Ethical Committee at Hokkaido University Graduate School of Medicine. Basic medium used in BMCS isolation and culture consisted of Dulbecco's Modified Eagle's Medium (DMEM; Nissui, Tokyo, Japan), 10% lot-selected fetal bovine serum (FBS) (Invitrogen Corp., Carlsbad, CA USA), and 100 units/ml of penicillin G (PCG) (Banyu Pharmaceutical Co., Ltd., Tokyo, Japan). To harvest mice BMSC, the femurs were aseptically dissected from female ICR mice (6–8 weeks). After both ends of the femurs were cut, whole bone marrow was extruded with 5 ml of basic medium containing 500 units of heparin, using a 2.5-ml syringe and a 21-gauge needle. Whole marrow cells were then centrifuged at 2 × 103 rpm for 5 min at 15 °C, and the supernatant was discarded to remove debris. Pelleted whole marrow cells were diluted with 25 ml of basic medium and seeded on a 150-cm^2 collagen I-coated flask (Becton Dickinson Labware, Bedford, MA) at 37.0 °C, 5% CO_2. After 24 h, non-adherent, floating cells including hematopoietic cells and debris were removed by changing the medium. Remaining cells that adhered to the flask bottom were incubated with the basic medium and were passaged before reaching confluence (Lee et al., 2003; Shichinohe et al., 2004). Cells were utilized for subsequent experiments after 3 passages.

4.2. *Protocol of "chemical induction"*

The BMSC were seeded on fibronectin-coated 4-well culture (1.7 cm^2 per well) slides and 75-cm^2 flasks (Becton Dickinson Labware, Bedford, MA) at a density of 2.9×10^4 cells/cm^2. After seeded cells were confirmed to be viable and adherent to the bottom of the slide or the flask, basic medium was discarded and was replaced with an induction medium consisting of DMEM, 10% FBS, 100 units/ml of PCG, 2% dimethylsulfoxide (DMSO) (Wako Pure Chemical Industries, Ltd., Osaka, Japan), 10-ng/ml basic fibroblast growth factor (bFGF) (R&D systems Inc, Minneapolis, MN), and 10-μM all-trans retinoic acid (RA) (SIGMA, Saint Louis, Missouri). The induction medium was changed once 3 days later. The induction treatment was completed after 5–6 days. As a control, a subculture of BMSC was incubated with basic medium in parallel with those in induction medium. The cells on the 4-well culture slides and 75-cm^2 flasks were processed for immunocytochemistry and RNA extraction, respectively. The cells in the culture slide or flask were visualized with an Olympus CK2 inverted microscope (Olympus, Tokyo, Japan) and were digitally photographed with a CAMEDIA C-4040ZOOM camera (Olympus, Tokyo, Japan).

4.3. *Immunocytochemistry*

After discarding the medium, the cells on the culture slide were rinsed twice with phosphate-buffered saline (PBS). The cells were fixed with 4% acetone for 3 min and then immersed in PBS for 10 min. For blocking non-specific immune reaction, the cells were treated with 10% goat serum for 30 min. Primary antibodies used in this study are mouse monoclonal anti-nestin (1:200, Chemicon, Temecula, CA), rabbit polyclonal anti-neurofilament M (1:200, Chemicon), and mouse monoclonal anti-tubulin, beta III isoform (Tuj 1) (1:200, Chemicon). According to the manufacturer's protocol, each primary antibody was diluted and incubated 1 h with secondary antibody, Zenon™ One Alexa Fluor 488 mouse IgG_1/rabbit IgG labeling kits (Molecular Probes, Inc. Eugene, OR). Then the cells were rinsed twice for 10 min with cold PBS. The cells were visualized and digitally photographed with a fluorescence microscope BX51 (Olympus, Tokyo, Japan) and a digital microscope system VB-6000/6010 (Keyence, Osaka, Japan).

For quantification, the cells that showed specific immunolabeling were counted in six randomly selected fields at a magnification of 200×.

4.4. *Microarray analysis*

Both untreated and treated BMSC were detached from the flask with 0.25% trypsin/0.02% EDTA in PBS. Cells were pelleted by centrifugation, and total RNA was extracted from the pellet using an RNeasy Mini Kit (Quiagen, Chatsworth, CA), according to the manufacturer's recommendations. Gene expression profiles of the untreated and treated BMSC were assessed using oligoDNA microarray, CodeLink UniSet™ Mouse 20 K I Bioarray (Amersham Biosciences Corp., Piscataway, NJ), which contained approximately 20,000 known mouse genes, 300 negative control genes, and 100 positive control genes. Two sets of total RNA solutions, derived from untreated and treated BMSC, in RNase-free water were submitted to Kurabo Industries Ltd. (Osaka, Japan) and processed for microarray analysis. Briefly, RNA quality was checked, and first-strand cDNA was synthesized using 2 μg of total RNA. Then, second-strand cDNA was synthesized. The resultant double-strand cDNA was purified, and cRNA was synthesized by in vitro transcription. After recovery and fragmentation of biotin-labeled cRNA, the target cRNA was hybridized to the probe on the array. After post-hybridization wash, streptavidin-dye was conjugated, and the array was scanned and analyzed. Fluorescence on the bioarray was scanned with GenePix™ 4000B (Axon Instruments Inc., Union City, CA), and the signal was analyzed with CodeLink System Software Version 2.3 (Amersham Biosciences Corp.).

4.5. *Evaluation of the results of microarray analysis*

Both quantitative and qualitative data were output from the software. Both data were indicated as raw signal intensity and quality flags, respectively. Raw signal intensities were normalized by the following formula: normalized signal intensity = raw signal intensity of the interested gene / median of the raw signal intensities of the discovery probes, where the discovery probe represented a probe other than negative control probe (NCP) on the array. Quality flags were classified into "good", "empty", and "poor" by image analysis software. When the signal intensity was enough for analysis, the spot was judged as "good". When the signal intensity was not enough for analysis or could not be scanned by the software, the spot was judged as "empty". The spot was judged as "poor" when its shape was abnormal.

Output data of signal intensity were distinguished from the background signal. To gain a background signal threshold, the

Table 2 – Sequences of specific probes for RT-PCR

Gene title	Symbol (synonym)	Forward/Reverse	Primers sequences (from 5′ to 3′)	bp	Genbank accession #
Nestin	Nestin	Forward	AGCACGAGGCTGAGGTGCAGCG	506	NM_016701
		Reverse	CGCCTCTCTGCGTTCCTGGAG		
Tubulin, beta 3	Tubb3 (Tuj 1)	Forward	GTCAGCTCAATGCCGACCTCCG	559	NM_023279
		Reverse	GCAGTGGCGTCCTGGTACTGC		
Neurofilament 3, medium	Nef3 (NF-M)	Forward	CAGCCGCGTGAGCGGTTCC	534	NM_008691
		Reverse	CGAATGGCAGCCTCGGTGTCG		
Secreted acidic cysteine rich glycoprotein	Sparc	Forward	CGTCTGCGCATGCGTGACTGG	526	NM_009242
		Reverse	CCAGGCGGAACAGCCAACCATC		
Procollagen, type I, alpha 2	Col1a2	Forward	CCTCTGGAGAACCTGGTACCGC	476	NM_007743
		Reverse	CCTCGGATGCCTTGAGGACCAC		
Transgelin	Tagln	Forward	GGTCCATCCTACGGCATGAGCC	547	NM_011526
		Reverse	GCGAGGCTCCTCTGTTGCTGC		
Tropomyosin 1, alpha	Tpm1	Forward	GAAGGCGGCGGAAGACCGGAG	455	NM_024427
		Reverse	CCTCTGCACGTTCCAGGTCGCT		
Fibrillin 1	Fbn1	Forward	GCTGAGGTTGGCCATTCACGCC	535	NM_007993
		Reverse	GGAGGATGCGGTGGTGATCCTC		
Insulin-like growth factor 1	IGF1	Forward	CACCACAGCTGGACCAGAGACC	568	NM_010512
		Reverse	TAAACAAACACTCCTAAAGACGA		
Interleukin 6	IL6	Forward	CTGATGCTGGTGACAACCACGGC	505	NM_031168
		Reverse	GCCACTCCTTCTGTGACTCCAGC		
Brain-derived neurotrophic factor	BDNF	Forward	TGAAGAGCACAGACGGCTCCTGC	589	NM_007540
		Reverse	GCTGATGTCTCCTGTGAAGCCGC		
Glia maturation factor, beta	Gmfb	Forward	CCAGACTGCCGAGCTAACCAAGG	454	NM_022023
		Reverse	CCAGGAGTGGTCAGAGGAGGAAC		
Mus musculus ciliary neurotrophic factor, transcript variant 2	CNTF	Forward	CCCAGGAAGAGAGGGAGAAGGC	527	NM_053007
		Reverse	GCAATCAGCACCTCAGGGTGGC		
Nerve growth factor, bet	NGFb	Forward	GCCGCAGTGAGGTGCATAGCG	574	NM_013609
		Reverse	GGATTGGAGGCTCGGCACTTGG		
Transforming growth factor, beta 3	TGFb3	Forward	GTGCGCGAGTGGCTGTTGAGG	517	NM_009368
		Reverse	GGACGCAGCATGGCGAGGCA		
Actin, beta, cytoplasmic	Actb	Forward	TCCTATGTGGGTGACGAGG	245	NM_007393
		Reverse	TACATGGCTGGGGTGTTGAA		

top and bottom 10% of signal intensities of NCP were dismissed. Mean value of NCPs (MVNCP) was obtained from signal intensities of the residual 80% of NCPs. Background threshold was obtained by adding 3 standard deviations of MVNCP. A gene of interest was considered to be "expressed" when the signal intensity was above the background signal threshold and the quality flag was indicated as "good".

The difference of the gene expression between two samples (i.e., untreated and treated MSCs) was evaluated using a ratio of normalized signal intensities. The ratio was calculated as follows: a ratio is obtained by Y/X, where X is the normal signal intensity of the untreated BMSC, and Y is that of the treated BMSC, when normalized signal intensity of the treated BMSC was higher than that of the untreated BMSC. The gene of interest is then estimated to be up-regulated by the treatment. In contrast, a ratio is defined as –X/Y, when the normalized intensity of the treated MSCs was lower than that of the untreated MSCs. The gene of interest is then judged as down-regulated. When the ratio exceeds 2 or –2, the change in gene expression is determined to be significant.

In this study, we used gene symbols in the sublists of "the master list of stromal cell genes" as a key word for data mining (Seshi et al., 2003). Seshi et al. (2003) identified 2755 genes expressed in 23 samples of human BMSC using microarray analysis and published the list as an on-line Excel file (Seshi et al., 2003). They concluded that 251 out of the 2755 genes (9.1%) were associated with diverse cellular lineages and classified them into several sublists according to their cellular lineages (e.g., the list of osteoblast/bone cell/bone disorder-associated genes). Using the present data obtained from microarray analysis, in this study, we examined whether the untreated BMSC expressed any of the multilineage cellular genes listed in Seshi's sublists and whether in vitro "chemical induction" altered the gene expression profile of the BMSC.

4.6. RT-PCR

Total RNA used for cDNA synthesis was derived from the same samples that were submitted to microarray analysis. To synthesize cDNA, 0.3 μg of total RNA were added in a 12-μl volume containing 1 μl oligo(dT)$_{12-18}$ primer (Invitrogen), 4 μl of 2.5-mM dNTPmix, and distilled water. The mixtures were heated to 65 °C for 5 min and chilled quickly on ice. Then, 4 μl of 5× first-strand buffer, 2-μl 0.1 M DTT, and 1-μl ribonuclease inhibitor (Takara, Shiga, Japan) were added to the mixture. Mixed contents were incubated at 37 °C for 2 min. By adding 1 μl of M-MLV reverse transcriptase (M-MLVRT) (Invitrogen), reaction volume became 20 μl. The total mixture was incubated at 37 °C for 50 min, and the reaction was inactivated by heating at 70 °C for 15 min. In control reactions, M-MLVRT was omitted.

RT-PCR was performed to verify the data from the microarray. Microarray data were confirmed by RT-PCR, and representative genes were selected from our microarray analysis. Primer sequences (F: forward, R: reverse) and Genbank accession numbers are shown in Table 2. The total volume of the 50 μl reaction mixture contains 2 μl cDNA, 5 μl of 10× PCR buffer, 3 μl of 25 mM $MgCl_2$, 4 μl of 2.5 mM dNTPmix, 10 pmol of forward and reverse primer, 33.6 μl of distilled water, and 0.4 μl of Taq polymerase, TaKaRa Taq (Takara). The reaction mixtures were processed for PCR. Reaction temperatures were as follows: (1) to indicate altered gene expressions semiquantitatively: initial 2-min denature step at 94 °C followed by 22 cycles of 94 °C 30 s, 58 °C 30 s, 72 °C 1 min, 72 °C 5 min; (2) to confirm gene expressions in MSCs qualitatively: initial 5-min denature step at 96 °C followed by 33 cycles of 96 °C 40 s, 58 °C 30 s, 72 °C 1 min, 72 °C 5 min.

Acknowledgments

This study was supported by Grant-in-aids from the Ministry of Education, Science and Culture of Japan (No.14370424, Dr. Kuroda and No.15390426, Dr. Iwasaki) and by a grant from Mitsubishi Pharma Research Foundation (Dr. Kuroda). The authors deeply thank Ms. Yumiko Shinohe for her skillful assistance in cell culture and immunocytochemistry.

REFERENCES

Chen, J., Li, Y., Wang, L., Lu, M., Chopp, M., 2002a. Caspase inhibition by Z-VAD increases the survival of grafted bone marrow cells and improves functional outcome after MCAo in rats. J. Neurol. Sci. 199, 17–24.

Chen, X., Li, Y., Wang, L., Katakowski, M., Zhang, L., Chen, J., Xu, Y., Gautam, S.C., Chopp, M., 2002b. Ischemic rat brain extracts induce human marrow stromal cell growth factor production. Neuropathology 22, 275–279.

Chopp, M., Zhang, X.H., Li, Y., Wang, L., Chen, J., Lu, D., Lu, M., Rosenblum, M., 2000. Spinal cord injury in rat: treatment with bone marrow stromal cell transplantation. NeuroReport 11, 3001–3005.

Deans, R.J., Moseley, A.B., 2000. Mesenchymal stem cells: biology and potential clinical uses. Exp. Hematol. 28, 875–884.

Deng, W., Obrocka, M., Fischer, I., Prockop, D.J., 2001. In vitro differentiation of human marrow stromal cells into early progenitors of neural cells by conditions that increase intracellular cyclic AMP. Biochem. Biophys. Res. Commun. 282, 148–152.

Egusa, H., Schweizer, F.E., Wang, C.-C., Matsuka, Y., Nishimura, I., 2005. Neuronal differentiation of bone marrow-derived stromal stem cells involves suppression of discordant phenotypes through gene silencing. J. Biol. Chem. 280, 23691–23697.

Garcia, R., Aguiar, J., Alberti, E., de la Cuetara, K., Pavon, N., 2004. Bone marrow stromal cells produce nerve growth factor and glial cell line-derived neurotrophic factors. Biochem. Biophys. Res. Commun. 316, 753–754.

Jin, K., Mao, X.O., Batteur, S., Sun, Y., Greenberg, D.A., 2003. Induction of neuronal markers in bone marrow cells: differential effects of growth factors and patterns of intracellular expression. Exp. Neurol. 184, 78–89.

Kim, B.J., Seo, J.H., Bubien, J.K., Oh, Y.S., 2002. Differentiation of adult bone marrow stem cells into neuroprogenitor cells in vitro. Neuroreport 13, 1185–1188.

Kohyama, J., Abe, H., Shimazaki, T., Koizumi, A., Nakashima, K., Gojo, S., Taga, T., Okano, H., Hata, J., Umezawa, A., 2001. Brain from bone: efficient "meta-differentiation" of marrow stroma-derived mature osteoblasts to neurons with Noggin or a demethylating agent. Differentiation 68, 235–244.

Kopen, G.C., Prockop, D.J., Phinney, D.G., 1999. Marrow stromal cells migrate throughout forebrain and cerebellum, and they

differentiate into astrocytes after injection into neonatal mouse brains. Proc. Natl. Acad. Sci. U. S. A. 96, 10711–10716.
Lee, J.B., Kuroda, S., Shichinohe, H., Ikeda, J., Seki, T., Hida, K., Tada, M., Sawada, K., Iwasaki, Y., 2003. Migration and differentiation of nuclear fluorescence-labeled bone marrow stromal cells after transplantation into cerebral infarct and spinal cord injury in mice. Neuropathology 23, 169–180.
Lee, J.B., Kuroda, S., Shichinohe, H., Yano, S., Kobayashi, H., Hida, K., Iwasaki, Y., 2004. A pre-clinical assessment model of rat autogeneic bone marrow stromal cell transplantation into the central nervous system. Brain Res. Brain Res. Protoc. 14, 37–44.
Lou, S., Gu, P., Chen, F., He, C., Wang, M., Lu, C., 2003. The effect of bone marrow stromal cells on neuronal differentiation of mesencephalic neural stem cells in Sprague-Dawley rats. Brain Res. 968, 114–121.
Lu, P., Blesch, A., Tuszynski, M.H., 2004. Induction of bone marrow stromal cells to neurons: differentiation, transdifferentiation, or artifact? J. Neurosci. Res. 77, 174–191.
Mahmood, A., Lu, D., Wang, L., Li, Y., Lu, M., Chopp, M., 2001. Treatment of traumatic brain injury in female rats with intravenous administration of bone marrow stromal cells. Neurosurgery 49, 1196–1203 (discussion 1203-4).
Neuhuber, B., Gallo, G., Howard, L., Kostura, L., Mackay, A., Fischer, I., 2004. Reevaluation of in vitro differentiation protocols for bone marrow stromal cells: disruption of actin cytoskeleton induces rapid morphological changes and mimics neuronal phenotype. J. Neurosci. Res. 77, 192–204.
Ohta, M., Suzuki, Y., Noda, T., Ejiri, Y., Dezawa, M., Kataoka, K., Chou, H., Ishikawa, N., Matsumoto, N., Iwashita, Y., Mizuta, E., Kuno, S., Ide, C., 2004. Bone marrow stromal cells infused into the cerebrospinal fluid promote functional recovery of the injured rat spinal cord with reduced cavity formation. Exp. Neurol. 187, 266–278.
Prockop, D.J., 1997. Marrow stromal cells as stem cells for nonhematopoietic tissues. Science 276, 71–74.
Rismanchi, N., Floyd, C.L., Berman, R.F., Lyeth, B.G., 2003. Cell death and long-term maintenance of neuron-like state after differentiation of rat bone marrow stromal cells: a comparison of protocols. Brain Res. 991, 46–55.
Romero-Ramos, M., Vourc'h, P., Young, H.E., Lucas, P.A., Wu, Y., Chivatakarn, O., Zaman, R., Dunkelman, N., el-Kalay, M.A., Chesselet, M.F., 2002. Neuronal differentiation of stem cells isolated from adult muscle. J. Neurosci. Res. 69, 894–907.
Safford, K.M., Hicok, K.C., Safford, S.D., Halvorsen, Y.D., Wilkison, W.O., Gimble, J.M., Rice, H.E., 2002. Neurogenic differentiation of murine and human adipose-derived stromal cells. Biochem. Biophys. Res. Commun. 294, 371–379.
Sanchez-Ramos, J., Song, S., Cardozo-Pelaez, F., Hazzi, C., Stedeford, T., Willing, A., Freeman, T.B., Saporta, S., Janssen, W., Patel, N., Cooper, D.R., Sanberg, P.R., 2000. Adult bone marrow stromal cells differentiate into neural cells in vitro. Exp. Neurol. 164, 247–256.
Sekiya, I., Larson, B.L., Smith, J.R., Pochampally, R., Cui, J.G., Prockop, D.J., 2002. Expansion of human adult stem cells from bone marrow stroma: conditions that maximize the yields of early progenitors and evaluate their quality. Stem Cells 20, 530–541.
Seshi, B., Kumar, S., King, D., 2003. Multilineage gene expression in human bone marrow stromal cells as evidenced by single-cell microarray analysis. Blood Cells Mol. Dis. 31, 268–285.
Shichinohe, H., Kuroda, S., Lee, J.B., Nishimura, G., Yano, S., Seki, T., Ikeda, J., Tamura, M., Iwasaki, Y., 2004. In vivo tracking of bone marrow stromal cells transplanted into mice cerebral infarct by fluorescence optical imaging. Brain Res. Brain Res. Protoc. 13, 166–175.
Shichinohe, H., Kuroda, S., Yano, S., Onishi, T., Tamagami, H., Hida, K., Iwasaki, Y., 2006. Improved expression of gamma-aminobutyric acid receptor in mice with cerebral infarct and transplanted bone marrow stromal cells: an autoradiographic and histological analysis. J. Nucl. Med. 47, 486–491.
Terada, N., Hamazaki, T., Oka, M., Hoki, M., Mastalerz, D.M., Nakano, Y., Meyer, E.M., Morel, L., Petersen, B.E., Scott, E.W., 2002. Bone marrow cells adopt the phenotype of other cells by spontaneous cell fusion. Nature 416, 542–545.
Tremain, N., Korkko, J., Ibberson, D., Kopen, G.C., DiGirolamo, C., Phinney, D.G., 2001. MicroSAGE analysis of 2,353 expressed genes in a single cell-derived colony of undifferentiated human mesenchymal stem cells reveals mRNAs of multiple cell lineages. Stem Cells 19, 408–418.
Wieczorek, G., Steinhoff, C., Schulz, R., Scheller, M., Vingron, M., Ropers, H.H., Nuber, U.A., 2003. Gene expression profile of mouse bone marrow stromal cells determined by cDNA microarray analysis. Cell Tissue Res. 311, 227–237.
Woodbury, D., Schwarz, E.J., Prockop, D.J., Black, I.B., 2000. Adult rat and human bone marrow stromal cells differentiate into neurons. J. Neurosci. Res. 61, 364–370.
Woodbury, D., Reynolds, K., Black, I.B., 2002. Adult bone marrow stromal stem cells express germline, ectodermal, endodermal, and mesodermal genes prior to neurogenesis. J. Neurosci. Res. 69, 908–917.
Wu, S., Suzuki, Y., Ejiri, Y., Noda, T., Bai, H., Kitada, M., Kataoka, K., Ohta, M., Chou, H., Ide, C., 2003. Bone marrow stromal cells enhance differentiation of cocultured neurosphere cells and promote regeneration of injured spinal cord. J. Neurosci. Res. 72, 343–351.
Ying, Q.L., Nichols, J., Evans, E.P., Smith, A.G., 2002. Changing potency by spontaneous fusion. Nature 416, 545–548.
Zhong, C., Qin, Z., Zhong, C.J., Wang, Y., Shen, X.Y., 2003. Neuroprotective effects of bone marrow stromal cells on rat organotypic hippocampal slice culture model of cerebral ischemia. Neurosci. Lett. 342, 93–96.

Amyotrophic Lateral Sclerosis. 2006; 7: 38–45

Taylor & Francis
Taylor & Francis Group

ORIGINAL ARTICLE

Nationwide survey of juvenile muscular atrophy of distal upper extremity (Hirayama disease) in Japan

KUNIO TASHIRO[1], SEIJI KIKUCHI[1], YASUO ITOYAMA[2], YUKIO TOKUMARU[3], GEN SOBUE[4], EIICHIRO MUKAI[4], ICHIRO AKIGUCHI[5], KENJI NAKASHIMA[6], JUN-ICHI KIRA[7] & KEIZO HIRAYAMA[3]

[1]*Hokkaido University, Sapporo,* [2]*Tohoku University, Sendai,* [3]*Chiba University, Chiba,* [4]*Nagoya University, Nagoya,* [5]*Kyoto University, Kyoto,* [6]*Tottori University, Yonago, and* [7]*Kyushu University, Fukuoka, Japan*

Abstract

Juvenile muscular atrophy of the distal upper extremity (JMADUE, Hirayama disease) was first reported in 1959 as 'juvenile muscular atrophy of unilateral upper extremity'. Since then, similar patients in their teens or 20s have been described, under a variety of names, not only in Japan, but also in other Asian countries, as well as Europe and North America. Biomechanical abnormalities associated with JMADUE have recently been reported through various imaging examinations, proposing its disease mechanism. Since JMADUE differs from motor neuron disease, or spinal muscular atrophy, this disease entity should be more widely recognized, and early detection and effective treatments should be considered. We report an epidemiological study in Japan. Two nationwide questionnaire-based surveys, conducted in Japan from 1996 to 1998, identified 333 cases. The numbers of patients per year, distribution of ages at onset, mode of onset, time lapse between onset and quiescence, neurological signs and symptoms, imaging findings, and the effects of conservative treatments were analyzed. The peak age was 15 to 17 years, with a marked male preponderance, usually a slow onset and progression, and quiescence six or fewer years after onset. There was a predominantly unilateral hand and forearm involvement with 'cold paresis'. The imaging findings are described.

Key words: *JMADUE, Hirayama disease, epidemiology, cervical flexion myelopathy*

Introduction

Juvenile muscular atrophy of distal upper extremity (JMADUE), Hirayama disease, was first reported in 12 patients by Hirayama et al. in 1959 (1). Subsequently 20 cases were reported as juvenile muscular atrophy of the unilateral upper extremity (2). Hirayama distinguished this disease from previously known degenerative and progressive motor neuron diseases (3). Sobue et al. from Nagoya University, Japan, independently reported 71 cases of an identical disease in 1978, which they termed the juvenile type of distal and segmental muscular atrophy of the upper extremities (4). In India in 1984, Gourie-Devi and her group proposed the term monomelic amyotrophy (5). However, their paper included monomelic amyotrophy of not only the upper, but also the lower, extremity.

The first autopsy case was reported by Hirayama et al. in 1987 (6). The patient was a 38-year-old man who died of lung cancer in 1982. He had a history of muscle weakness involving the left hand beginning at age 15 years which was followed by atrophy, but became stable in about one year. Slight muscle atrophy of the right first dorsal interosseous muscle was noted at age 36 years. The pathological findings revealed antero-posterior flattening of the cord, predominantly at C7 and C8. Microscopically, the anterior horn cells were decreased in number, most severely at the C7 and C8 level and predominantly on the left, but the cord segments C5–T1 were also involved. The pathophysiological mechanism of this anterior horn cell loss was considered possibly due to a circulatory disturbance. In 1991, Hirayama designated this entity as Hirayama disease (7). Similar cases have been reported under a variety of names in other Asian countries: Loong (8) (Singapore, 1975), Singh (9) (India, 1980), Gourie-Devi (5) (India, 1984), Tan (10) (Malaysia, 1985), Virmani (11) (India, 1985), Peiris (12) (Sri Lanka, 1989), Chan (13) (Hong Kong, 1991), Kao (14) (Taiwan, 1993), Mirsa (15) (India, 1995), and Chen (16) (Taiwan,

Correspondence: K. Tashiro, Department of Neurology, Hokkaido University Graduate School of Medicine, Sapporo 060-8648, Japan. E-mail: tashiro@med.hokudai.ac.jp

(Received 24 November 2004; accepted 12 September 2005)

ISSN 1748-2968 print/ISSN 1471-180X online
DOI: 10.1080/14660820500396877

1998). Subsequently, cases have also been described in western countries: Pilgaard (17) (Denmark, 1968), Compernolle (18) (Holland, 1973), Adornato (19) (USA, 1978), O'Sullivan (20) (Austraia, 1978), Harding (21) (UK, 1983), Schlegel (22) (Germany, 1987), Leys (23) (France, 1987), Chaine (24) (France, 1988), Gaio (25) (France, 1989), Biondi (26) (France, 1989), Oreyma (27) (Canada, 1990), Donofrio (28) (USA, 1994), Billé-Turc (29) (France, 1996), Drozdowski (30) (Poland, 1998), and Shröder (31) (Germany, 1999).

Recently, Hirayama proposed the term 'juvenile muscular atrophy of distal upper extremity' (JMADUE); therefore, this term is used in this report (32–34).

Although the entity 'monomelic spinal muscular atrophy' is recognized in western countries, clinical classification of these various syndromes is not consistent in different countries. The pathogenesis of JMADUE is yet to be defined. However, the hypothesis that biomechanical factors acting on the cervical cord and dural sac during neck flexion might cause a cervical poliomyelopathy has been proposed (34–38).

Although upper limb muscular atrophy, due to motor neuron disease or spinal muscular atrophy, is known to occur in young persons, the progression and prognosis of these entities is entirely different from JMADUE, which is benign in clinical course and never fatal. In addition, early detection and treatment are effective in halting progression of JMADUE. Our epidemiological study in Japan provides an overview of the clinical features of this condition.

Subjects and methods

The clinical requirements we used for the diagnosis of JMADUE are summarized in Table I.

First survey

To determine the number of JMADUE patients, a survey form was sent to members listed on the rosters provided by the Japanese Societies of Neurology, Orthopedics, Neurosurgery and Child Neurology, requesting details of patients fulfilling the inclusion criteria shown in Table I. In this first survey, we tried to collect as many cases as possible based on the clinical diagnosis, irrespective of the availability of data from neuroradiological examinations. These first survey forms were mailed in June 1996.

Second survey

The second survey forms were mailed in June 1997 to those facilities that had reported having treated patients with this disease. In this survey, the items included requests for information on patients, their medical records, clinically observed neurological findings, neuroradiological findings, electromyographic (EMG) findings, treatments provided and their outcome. Receipt of responses to the second survey was closed in October 1998, and the collected data were analyzed. In the second survey, identifying information on individual patients was required, including name and birth dates. These data were required to identify duplicate reporting of patients provided by two or more hospitals or physicians. Ethical permission was obtained for this second survey from every participating institution.

Results

Results of the first survey

The first survey forms were mailed to 429 facilities with neurology departments, 2194 facilities with orthopedic departments, 998 facilities with neurosurgery departments and 199 facilities with child neurology departments; a total of 3820 facilities. Replies were received from 2260 facilities (59.16%). These replies reported 562 cases from 156 facilities.

Results of the second survey

The second survey forms were mailed to the 156 responding facilities, 54 of which returned the completed forms. In this way a total of 333 cases were identified, and these were used for our analysis. Two hundred and ninety of the 333 cases (87.1%) were reported from neurology departments. We considered that 247 of the 333 reported cases were 'definite', while 86 out of 333 were judged as having some atypical features based on the initially defined diagnostic criteria, although these were included in the total. Therefore, all these 333 cases were analyzed as JMADUE in this report.

Table I. Requirements for the diagnosis of JMADUE (Hirayama disease).

1. Distally dominant muscle weakness and atrophy in forearm and hand.
2. Onset between ages 10 years and the early 20 s.
3. Unilateral or unilaterally dominant symptoms and signs.
4. Insidious onset with gradual progression for the first several years, followed by arrest of progression.
5. Lack of sensory disturbance and tendon reflex abnormalities, and no symptoms or findings in the lower extremities.
6. Other diseases (such as syringomyelia, spinal cord tumors, ossification of posterior longitudinal ligament, cervical spondylosis, other cervical vertebral abnormalities, motor neuron disease, motor neuropathy) must be excluded.

Only a few cases per year were reported prior to 1976, but in the 1980s the number of cases exceeded 10 per year, then after 1987 it rose to 20 or more. The relatively small number after 1995 reflects partial case discovery, since the inquiries were sent out in 1996 and 1997 (Table II). The average age at onset is about the same in each year (Table III). Although the average age of patients seeking first neurological consultation for this condition varies slightly by year, the overall tendency is for the age at onset to be under 25 years. Distribution of ages at onset and ages of patients at first neurological examination are shown in Table III and Figure 1. Signs and symptoms related to this disease appear at the age of 15 to 17 years in 53.4% of all patients; the peak of their first medical examination is 17 to 18 years.

There was a marked male preponderance, with 281 males to 34 females. Females account for only 10.8% of JMADUE patients. For females, onset was slightly older (mean 19.3 years) than for males (mean 17.6 years), but the difference in age of onset in males and females was not statistically significant. With regard to disease progression, there were 275 patients in whom the disease progressed slowly, 36 cases somewhat more quickly, and only three cases progressed rapidly.

Table II. Number of cases by year of onset.

Year	Number of cases on onset	Year	Number of cases on onset
1941		1975	2
1942	1	1976	2
1947	1	1977	12
1950	1	1978	7
1951	1	1979	7
1955	1	1980	13
1956	3	1981	12
1957	2	1982	12
1958	3	1983	7
1959	4	1984	13
1960	1	1985	6
1961	1	1986	11
1962	2	1987	21
1964	2	1988	23
1965	1	1989	30
1966	6	1990	22
1967	3	1991	18
1968	2	1992	19
1970	3	1993	19
1971	2	1994	10
1972	3	1995	6
1973	5	1996	3
1974	5	1997	

Table III. Average age at onset, and average age of patients at first medical examination by year.

Year	Average age at onset	Average age of patients at first medical examination
<1954	15.8	20
1955-1959	16.5	-
1960-1964	18.2	20.7
1965-1969	16.5	17
1970-1974	16.3	19.8
1975-1979	17.5	21.1
1980-1984	16.9	23.2
1985-1989	18.3	24.2
1990-1994	17.3	21.9
1995<	22.3	25.1

Period of disease progression

In cases in which the disease became quiescent the time lapse between onset and quiescence was less than three years in 69.7% of the cases, and less than six years in 90.8% (see Figure 2). The disease stopped progressing before age 25 years in the majority of cases (see Figure 3).

Neurological findings (Table IV)

The disorder usually commenced in the right hand regardless of handedness. JMADUE signs commenced unilaterally in 72.1% of patients, bilaterally but somewhat asymmetrically in 24.8%, and symmetrically in only 3.1%. Muscular atrophy was observed in the hands of 98% of patients. It was predominant on the ulnar side of the forearm in 88.7% of patients. There were also cases in which muscular atrophy was noted in the brachioradial muscle (18.2%), biceps brachii (8.8%), and triceps brachii (17.3%). The term 'cold paresis' refers to marked weakness of fingers occurring with exposure to cold, as described by Hirayama (39). When it appeared as the first symptom of JMADUE, there was often a history that muscular strength decreased only in the wintertime, but became chronic over time and then persisted throughout the year. Trembling of the fingers was noted when the fingers were extended. Both cold paresis and trembling of the fingers were noted in the majority of cases. Hirayama et al. (39) conducted a 'cold paresis inducement test' and showed by EMG that cold paresis was caused by conduction block of the muscle fiber membrane in re-innervating muscles after active denervation. It was not due to autonomic dysfunction (39). Although sensory disturbances were reported, they were only slight in degree. The tendon reflexes were reduced in the upper limbs, sometimes with hyperreflexia in the lower limbs. A Babinski sign was reported in very few cases. Two apparently familial cases were reported in two pairs of brothers. There were two other cases that were judged 'probable' familial cases.

Pathological (biopsy) findings

Pathological (biopsy) findings were reported in 21 cases, four of which were cervical dural biopsies, and the rest muscle biopsies. Microscopically, neurogenic atrophy of muscles, and decreased elastic fiber